Wearable Non-invasive Optical Body Sensor for Measuring Personal Health Vital Signs.

Zachary Joel Valentino Cohen

Wearable Non-invasive Optical Body Sensor for Measuring Personal Health Vital Signs.

By

Zachary Joel Valentino Cohen

Supervisor: Dr Shyqyri Haxha

A thesis submitted to the University of Bedfordshire, in fulfilment of the requirements for the degree of Masters of Science by Research

January 2016

Author's Declaration

I declare that this thesis is my own work. It is being submitted for the degree of Masters of Science by Research at the University of Bedfordshire.

It has not been submitted before for any degree or examination in any other University.

Name of candidate: Zachary Cohen

Signature:

Date: 7th January 2016.

i. Abstract

In this thesis, we report the development and implementation of healthcare sensor devices integrated into a wearable ring device. Using photoplethysmography (PPG) methods, we design a heart rate monitor, a unique method to measure oxygen saturation in the blood and discuss a potentially new method of continuous measurement of blood pressure. In this thesis we also report implementation of a temperature sensor using an LM35 transistor to measure body temperature. A method of integrating electrocardiography into the proposed device is also presented.

ii. Acknowledgments

The completion of this thesis could not have been possible without my superlative Director of Studies Shyqyri Haxha. His encouragement and intellectual support throughout my research degree has made me thoroughly enjoy undertaking my Masters of Science by Research degree.

I would also like to thank my wonderful family Amelia Dorian, Christopher Dorian, Rebecca Gershon, Joshua Gershon, Talulah Gershon, Jonas Gershon, Georgina Cohen and Emilio Giordano for the endless support throughout all of my endeavours. I would also like to acknowledge my fabulous grandparents Ruth Cohen, Sydney Cohen, Ruth Goldstein and David Goldstein. I would especially like to acknowledge Mitchell Cohen and Simone Cohen, my incredible father and mother who have supported me with everything I have ever done.

iii. Contents

i. Abstract i

ii. Acknowledgments ii

iii. Contents iii

Chapter 1 1

1.0 Introduction 1

1.1 Thesis Aim 2

Chapter 2 3

2.0 Background Research on Ring and Watch Technologies 3

2.1 The advantages of ring technologies over an embedded sensor watch. 3

2.2 Current Technology 4

Chapter 3 7

3.0 Heart rate 7

3.1 Heart Rate Introduction 7

3.2 Heart Rate Background Research 7

3.3 Heart Rate Implementation 9

3.4 Heart Rate Conclusion 16

Chapter 4 18

4.0 Body Temperature 18

4.1 Body Temperature Introduction 18

4.2 Body Temperature Background Research 18

4.3 Room Temperature Testing 19

4.4 Body Temperature Implementation 19

4.4 Body Temperature Conclusion 22

Chapter 5 23

5.0 SpO2 23

5.1 SpO2 Introduction. 23

5.2 Spectroscope measurement of SpO2 27

5.3 Spectrometer measurements, results and discussions 29

5.4.0 Measuring SpO2 with a TCS3200 colour sensor 34

5.4.1 Ring device results 36

5.4.2 Making the SpO2 device wireless 40

5.5 SpO2 Conclusion 44

Chapter 6 46

6.0 Blood Pressure 46

6.1 Blood Pressure Introduction 46

6.2 Blood Pressure Background Research 47

6.3 Blood Pressure Implementation 48

6.4 Blood Pressure Conclusion ..... **Error! Bookmark not defined.**

Chapter 7 64

7.0 Electrocardiography 64

7.1 Electrocardiography Introduction 65

Chapter 8 67

8.0 Conclusion 67

Publications: ..... **Error! Bookmark not defined.**

Chapter 9 68

9.0 Future Work 68

Chapter 10 71

10.0 Appendices 71

10.1 Appendix 1 71

10.2 Appendix 2 76

10.3 Appendix 3 ..... **Error! Bookmark not defined.**

10.4 Appendix 4 ..... **Error! Bookmark not defined.**

Chapter 11 78

11.0 Bibliography 78

Chapter 1

1.0 Introduction

As we live in a technological age where electronic devices are becoming more personal and more affordable, it is possible to give information to users without invading their personal security or privacy. Sensors that measure the body's basic functions (vitals), have been around for many years and are used every day. A heart rate monitor has been readily available for many years and due to the progression of technology, can enable us now to have such devices in our homes or even on us whilst we exercise. This work thesis will focus on wearable body sensors that will be able to measure health vitals and will also assess variables such as accuracy, affordability, reliability and the user interaction with said devices.

Medicine aims to find health problems in patients prior to symptoms occurring. It is possible to predict a heart attack months before it happens. Knowing a patient is at a high risk of having a heart attack could lead to prevention as a change in diet or habits for the patient could be implemented. Body sensors, able to view certain vitals of the patient could show advance signs of heart disease or angina (for example) and a patient could be warned to change their lifestyle to prevent any lasting damage to their health.

Body sensors, able to monitor a patient's vitals over a long period of time, can be put together to predict such problems that patients may face. Knowing a patient's personal information, inter alia, gender, weight and age could lead to the data being smarter. If we know the average heart rate of many thirty five year old females that are of average weight, we can predict the average heart rate of such a person. A heart rate well above or below the average could then be closely monitored and scrutinised to guard the patient if she is at any risk of heart problems.

The vitals that will be under scrutiny will be; heart rate, temperature, pulse oximetry, blood pressure and Electrocardiography (ECG).

1.1 Thesis Aim

This thesis is focused on producing and implementing non-invasive optical sensors that will be able to read a user's heart rate, body temperature, and oxygen saturation levels. The thesis will discuss a method of finding blood pressure with use of the thesis' heart rate monitor and introduce a way of implementing electrocardiography within the proposed ring device. The sensors will be introduced into a ring device for a medical examiner to be able to view a patient's recent health history. The thesis will focus on photoplethysmography (PPG) as a method of measurement in some of the devices.

Chapter 2

2.0 Background Research on Ring and Watch Technologies

This chapter will introduce the some health focussed devices currently available for consumers and discuss why the proposed thesis will produce a ring instead of a watch.

2.1 The advantages of ring technologies over an embedded sensor watch.

Many non-invasive health care devices use the techniques of photoplethysmography (PPG). PPG is a way of finding volumetric measurements with the use of light emitting diodes (LEDs) and phototransistors or photodiodes/light dependant resistors (LDR). These techniques which will be discussed further help to find the absorption of light at the photodetectors and is used to find vitals such as heart rate and oxygen saturation level.

Watches are the typical commercially available devices that use PPG techniques to find the heart rate and/or oxygen saturation levels of the user. There are two ways of obtaining the measurement with different positions of the components. The first is to place the LEDs and a photodetector next to each other. This is known as reflective mode and can be applied to most parts of the body surface [1]. The second methods is the transmissive mode which placed the LEDs and photo receiving sensor on the other side of the body [2]. This is mainly used within oxygen saturation monitoring devices where the photo sensor measures the change in absorbance through the extremity of a user on such places, inter alia on the earlobe, finger or toe. Placing such technology in watches leads to the reflective mode being used on the wrist where there is much light penetration needed to reach the appropriate arteries and reflect back to the sensor. This method is more unreliable and can lead to inaccurate results.

As a finger has a smaller cross sectional area compared to a wrist, this thesis will propose a ring with integrated sensors to find the heart rate, oxygen level, temperature and potentially blood pressure with main focus on the transmissive mode method.

There are a number of commercially available watches and bracelet based applications as will be discussed later but a ring would be more conducive and efficient as the finger has a smaller area thus produces a more accurate reading. This is because of the cross sectional areas of the body that they each cover. The average circumference of a female's finger is between 4.9cm and 5.7cm, giving a cross sectional area of 2.0cm^2 to 2.60cm^2. A male's average cross sectional area is between 2.60cm^2 to 3.60^2[3].

The average circumference of a female's wrist is between 15.2cm and 17.8cm (4.85cm in diameter); a male's between 17.8 and 20.3cm (5.7cm in diameter). This gives a female's average cross sectional area of a wrist of between 18.5cm^2 and 25.2cm^2 and a male's average cross sectional area of a wrist between 25.2cm^2 (5.7cm diameter) to 32.9cm^2 (6.5cm in diameter) as shown in table 1.1. Where ALA is average low area, AHA is the average high area, ALD is the average low diameter and AHD is the average high diameter.

	Ring				Wrist			
	ALA (Cm^2)	AHA (Cm^2)	ALD (Cm^2)	AHD (Cm^2)	ALA (Cm^2)	AHA (Cm^2)	ALD (Cm^2)	AHD (Cm)
Male	2.6	3.6	18.2	21.4	18.5	25.2	4.9	5.7
Female	2.0	2.6	15.8	18.2	25.2	32.9	5.7	6.5

Table 1.1. A table of the average areas of male and female fingers.

2.2 Current Technology

There are many different types of health watches presently available and many people buy such monitors to use during exercise. A heart rate monitor is useful during exercise as it allows the user to know if they need to train harder or indeed less hard. A recent experiment gathered some wristbands with heart rate monitoring capabilities and compared the results to an accurate benchmark ECG chest strap [4]. The results concluded many of the heart rate wrist monitors were inaccurate during exercise. Some couldn't even take a reading due to movement and when they

did, gave inconsistent results. The Basis Carbon Steel wristband cost £125, had an error ratio at rest of 10.2% and, even worse, an error ratio after exercise of 57.9%. It didn't work at all during exercise. It may have been aesthetically pleasing but the technology was clearly unreliable. The Withings Pulse Ox cost £95, had an error ratio of 5.3% at rest and a significant error ratio of 57.1% after exercise. The most expensive of the tested heart rate monitors was the Samsung Gear Fit at £169. It was not specifically aimed at the heart rate monitor market but also acted as a chain between wristband and smart phone via Bluetooth on the bracelet. The error ratio during rest was a reasonably accurate 4.2% but couldn't take a reading during the high heart rate produced by exercise. This was surprising as the most accurate monitor tested was the Samsung Galaxy S5 phone, working alone through touching the device with a finger, gave an error ratio, at rest, of just 3.1% and even better, 0.2% at a heart rate between 160-170 bpm after exercise. Since it is during exercise many users would require the knowledge of the heart rate, the wrist band devices would be rendered pointless and of questionable actual and economic benefit.

Further, watches are often worn as fashion or social statement. Many wear watches that have been passed to them as an heirloom. Whilst a watch may be changed and worn only for exercise this would defeat the stated object of continuous and regular measurement of vitals.

The proposed ring device will benefit all users though will be aimed at the elderly generation due to the likelihood of needing a continuous analysis of their vitals. The ring will be designed for use at the home for continuous vital measurements.

As the sensor is aimed at elderly and patients with brain disorders including dementia; the user may find it difficult to navigate the menus that form the watch profile. This could lead to the user feeling apathetic towards the watch and cause them to ignore the necessary functions leading to loss of data.

The ring will do all of the work for the user; the only interaction needed with the ring would be to put it on. The rest is up to the operator to check vitals and do what is necessary without any further input from the user. As the ring can notify the user (or a chosen nominee) if there is a problem with the user's vitals, it would reduce

the anxiety in the user. If the user hasn't received a message, then they may assume that their vitals are fine and thus will not be required to checking their device every time they don't feel as well as they might.

Chapter 3

3.0 Heart rate

Heart rate is arguably the most important of all vitals to monitor. Our heart rate changes during the whole day and can show medical experts what is happening with the patient's health. This chapter will discuss and produce a heart rate monitor ring device.

3.1 Heart Rate Introduction

When one is at rest, the average heart rate ranges from 60 to 100 beats per minute [5]. During sleep apnoea, there is a lack of air coming into the body, as a result, Oxygen levels decrease. If oxygen levels decrease below 90%, the patient gets into a state of hypoxemia. As a result of less oxygen flowing around the body, the heart rate increases. Detecting the rise in heart rate during an episode of sleep apnoea would allow to a potential to ameliorate the sleep apnoea episode if a detecting device could assist the patient. This chapter will discuss how heart rate monitors work and how to produce an appropriate heart rate monitor for the ring device.

When the heart is in systole (pumping the blood through the arteries), there is a change in blood flow within the arteries and therefore a pulse can be deciphered. A heart beat can be found by using an Infrared (*IR*) Light Emitting Diode (*LED)* that will send light through the arteries and will reflect some back. When the heart is in systole, the blood absorbs more light and thus less IR light will be reflected towards a phototransistor. As there are many capillaries within a finger, it is possible to get an accurate heart rate reading. The heart rate can also be detected from a Light Dependant Resistor (*LDR*) via an ultra-bright LED. The ultra-bright LED will produce more light than an IR LED and thus, more light will reach the LDR causing less resistance resulting in a higher output voltage.

3.2 Heart Rate Background Research

The current health related technologies on sale to the public are extremely expensive and don't provide full vitals and instead concentrate on heart rate. There are many watches that are typically incorporated with other non-health devices the

company has. For example, the Apple Watch can measure heart rate. Its starting price for the smallest watch is £300 and requires an iPhone for connectivity. It records a heartrate reading every ten minutes though not if the user's arm is moving [6]. As it is considered an aid to exercise this defeats its purpose since, it will not measure the heart rate if the user is running (and thus moving his arms) unless the user interrupts their run. Further, the watch will not record heart rate if the skin perfusion in the user's wrist is too low meaning that the watch will not measure the heart rate in cold weather. Furthermore, if the user has a tattoo where the watch is worn, it will also not be able to detect the heart rate and this necessitates the user using a compatible chest strap (at an extra cost of £80).

There are many external health related devices that can be connected to the Apple Watch including scales (£110), blood pressure monitor (£110) and a smart sleep system (£250) [7]. The smart sleep system is a device that is put under the mattress. It doesn't measure and vital information but does give the user lights and sounds 'scientifically proven' to help the user fall asleep and wake up rested at just the right time in the sleep cycle. It is contended that this extremely expensive watch and other devices can't measure anything of use for the user.

Probably the best health monitoring device presently available on the market would be the Fitbit. There are currently six different devices that Fitbit have produced ranging in prices from £50 to £200[8]. The more affordable Fitbit monitor is the Zip. The Zip is a glorified pedometer that can measure the steps taken, calories burned, distance travelled and 'active minutes' (how long the user has been active for). At the higher end of the spectrum, Fitbit's Surge device claims to be able to measure many beneficial exercise data such as; the amount of steps the user has taken, calories burned, floors climbed, 'active minutes', a sleep tracker and can measure a continuous heart rate [9]. Out of all of the data the smart watch can collect, only the heart rate could possibly be considered a notable vital that would be useful for health professionals allowing them to view the user's heart's changes over a lengthy period of time. Inputting your personal information to Fitbit's database is said to enable a user to see how healthy they are compared to the average person of their age and sex.

Accuracy tests were produced on the Fitbit Surge to see how accurate the heart rate monitoring device was. A runner wore a Fitbit watch and an additional accurate heart rate chest strap for later comparison as a bench mark device. The runner was monitored on a 45 minute run. The results showed that it took in the region of 8 minutes for the heart rate device to find the correct heart rate and was only within 82% of the real heart rate for the rest of the experiment [10].

Microsoft has developed a health band. It is called the Microsoft Band and costs £170. It can measure heart rate, deduce calories burned and measure sleep quality. The band can also connect to the user's smart phone (of any platform) and allow the user to have access to their phone's email and texts via the band. The band measures the user's heart rate depending on what the user is doing at the time [11]. If the user has set the band on 'exercise mode', the monitor records every second. During sleep, the monitor records the heart rate for two minutes, stops for eight and then repeats the cycle until the user has awoken. During the day, when the user is not exercising, the band records the heart rate for one minute, stops for nine and then repeats the cycle until the user has chosen a different mode [12]. A study has shown that the Microsoft Band is unreliable and inaccurate [13]. The test showed a benchmark EKG strap's heart rate to be 168 bpm where the Microsoft Band gave the result of 99bpm. This is a huge problem as 99bpm could be considered normal and 170 to be very high. If the user was at home with a high heart rate and the band though it was at a steady level, it would not be able to produce an alarm to a concerned practitioner.

These wrist bands show that the companies have rushed into producing devices that could prove harmful for the patient due to their unreliable and inaccurate measurements.

3.3 Heart Rate Implementation

The device needed to monitor the pulse combines a LDR and an LED, the microcontroller will be able to read the voltage output of the resistance from the LDR placed in series with a 10KΩ resistor as shown in Figure 3.1a below. The LDR and LED are placed within an elastic material for the comfort of the user, stimulate a greater pulse and allow the LDR to ignore any ambient light.

3.1. a 3.1. b

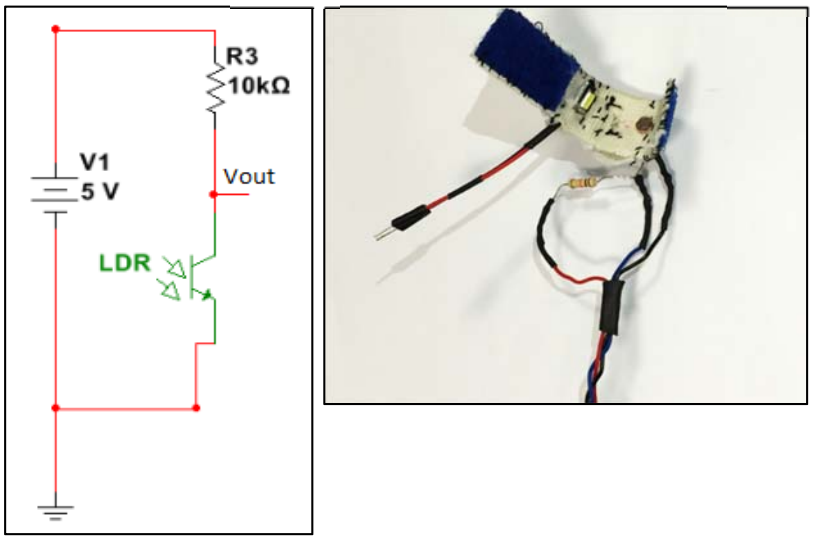

Figure 3.1.a. Circuit design for the LDR. 3.1. b. Real implementation of LDR circuit with LED enclosed in the elastic material held to the finger by Velcro.

When the circuit output is displayed on an oscilloscope, there is a visible rise in voltage as the heart beats. As there is more blood within the capillaries of the finger, less light reaches the LDR. As less light reaches the LDR, a higher resistance is recorded by LDR. As voltage is proportional to resistance in Ohm's law, a higher voltage is achieved. The output of the heart rate viewed from the oscilloscope is very 'fuzzy' and the oscilloscope has to be placed in the 20mV setting to view a 10mV change in heart rate. The heart rate has to be filtered and then amplified to be seen from the oscilloscope at an appropriate level for a microcontroller to be able to read.

When the signal is received, there is a large DC offset of ~2V. This disrupts the analogue reading and becomes negligible once amplified. The DC offset must be removed prior to amplification by filtering the input signal.

A suitable heart rate monitor should be able to read a heart rate across a high range. The chosen range of this heart rate monitor will be from 60 beats per minute (BPM) to 200BPM. A band-pass filter can be implemented to filter out any other unwanted frequencies and remove the unwanted DC offset. This is made up of a High Pass and a Low Pass filter.

A high-pass filter will eliminate any unwanted low frequencies and will use a 10KΩ resistor. As the lowest reading needed is 60BPM, we know that the frequency needed is 1HZ (1 beat per second). By using the formula (3.1), we can deduce the capacitance needed with the 10KΩ and 1Hz from information we already have.

$$C = \frac{1}{2\pi Rf} \quad (3.1)$$

The capacitance needed is 15.9µF. There is no commercially available 15.9 real capacitor, but we can use a 4.7µF capacitor in parallel with a 10µF capacitor to produce 14.7µF. By using 14.7 µF instead of 15.9, we will be cutting off frequencies below 1.08Hz (~65BPM). This is still acceptable for the heart rate monitor and can be seen in Figure 3.2 below.

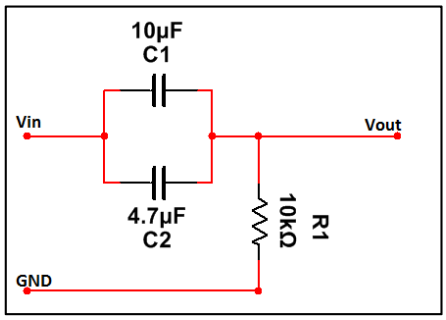

Figure 3.2. High pass filter design circuit.

Now that the high-pass filter has been implemented, a low-pass filter can be designed to cut off the frequencies higher than the wanted frequencies. The highest frequency needed is 3.3Hz (200 BPM). By using the same equation (3.1), where the same resistance of 10KΩ and a frequency of 3.3Hz, we can calculate the low-pass filter's capacitance value. The capacitance needed is 4.8µF. Again, there is no 4.8µF capacitor available but a 4.7µF which can be used instead. This gives an overall low-pass cut off frequency of 3.38Hz (203BPM) as shown below in Figure 3.3.

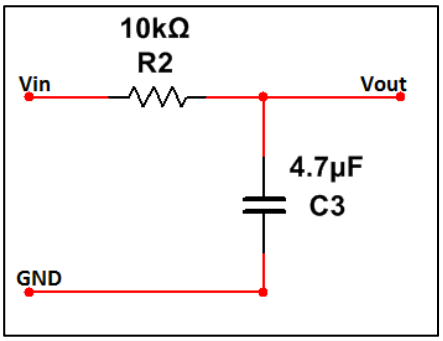

Figure 3.3. Low pass filter circuit design.

The second order band-pass filtering design is completed with a high-pass filter of 10KΩ resistance and 14.7µF capacitor to cut off 1.08Hz and a low-pass filter of resistance 10KΩ and capacitance of 4.7µF to cut off 3.38Hz giving an overall centre frequency of;

$$fr = \sqrt{fl \times fh} \qquad (3.2)$$

This makes the centre frequency 1.91Hz. The overall high pass to low pass filter design is shown below in Figure 3.4.

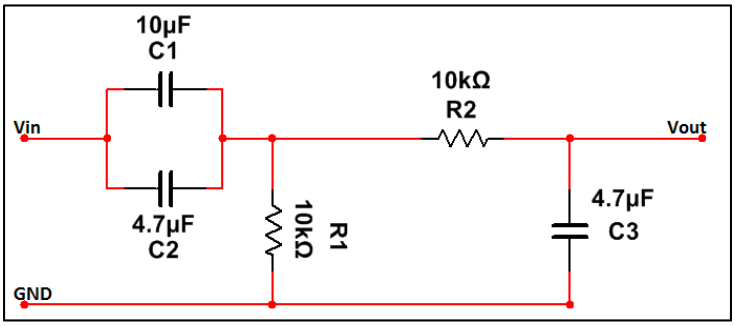

Figure 3.4. High pass to low pass filter design.

As filtering is complete, and the oscilloscope's output has a smooth analogue line, amplification is the next stage to produce a higher output.

During filtering, the DC-offset is now absent which is ideal as the AC voltage is the one that needs to be amplified. An LM386 OP-AMP requires 6V and produces a gain of 20. As the output is 20mV, we can expect a 0.4V out of the OP-AMP. The OP-AMP's circuit design is shown below in Figure 3.5, where IN- (pin 2) is grounded and IN+ is the output of the second order band-pass filter.

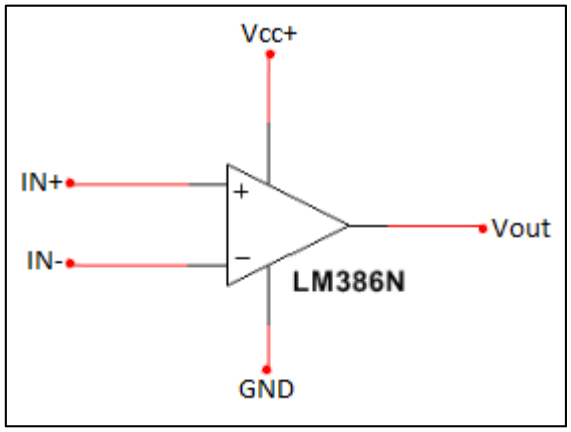

Figure 3.5. LM386 OP-AMP

The oscilloscope now produces a 0.2V output when the heartbeat is made. A resistor and capacitor can now be added again to smooth the output and diminish the DC off-set produced by the LM386 OP-AMP. The circuitry design was implemented on a breadboard which produces a lot of capacitance. A printed circuit board (PCB) was made for the circuit and the components soldered on as shown in Figure 3.6.

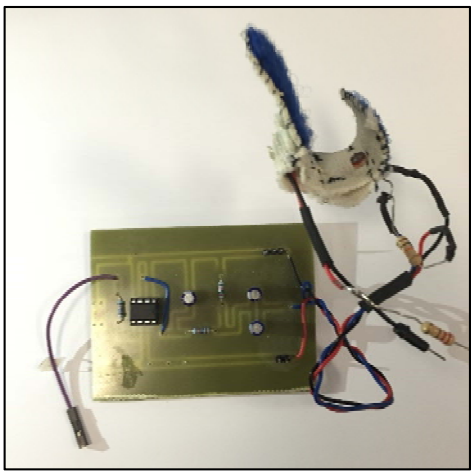

Figure 3.6. PCB circuit with LDR sensor ring, filters, OP-AMP and Vout.

Now that the heart beat can be seen, filtered and amplified, it is time to begin the programming to tell the microcontroller what a heartbeat is and how to find the heart rate per minute. An Arduino UNO was used as it has the libraries required and is easily programmed. The Arduino read the output of the heart rate monitor in an analogue form from 0-1023. As the Arduino's voltage at analogue read of 0 is 0v and an analogue read of 1023 is 5V, it is easy to convert the reading into the voltage (Voltage = analogue reading × (5 / 1023)). A spreadsheet was produced which recorded the output voltage against time (one voltage reading every 50ms).

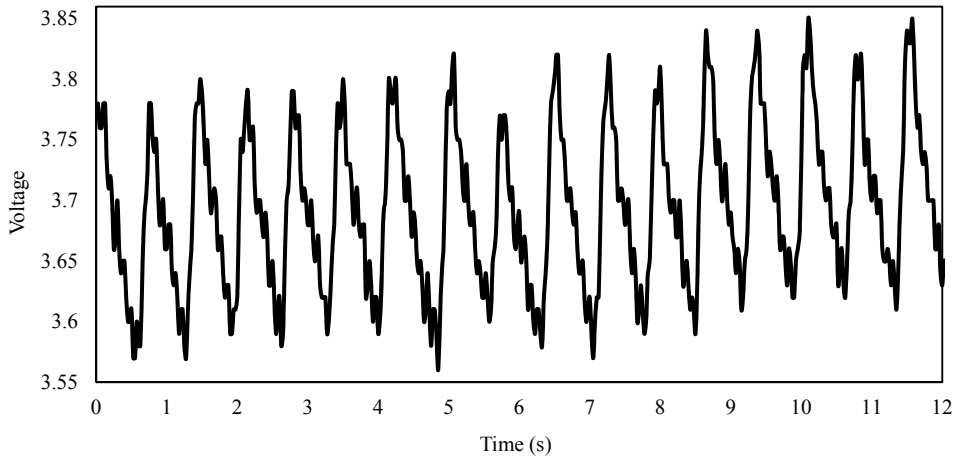

Figure 3.7 Graph of output of LDR sensor against time.

It is clear to see that there is a change in voltage as the heart is pumping. Figure 3.7 shows 17 pulses in 12 seconds (0.2 minutes) This would give a heart rate of 85BPM (17/0.2).

A closer look at the results from one heartbeat, shown in Figure 3.8 can show that the maximum voltage (grey line) is at 3.80V and the minimum at 3.57V. This gives an overall voltage of 0.25V per beat with the average being ~3.69V. When the reading is above the average 3.7V, a pulse is present.

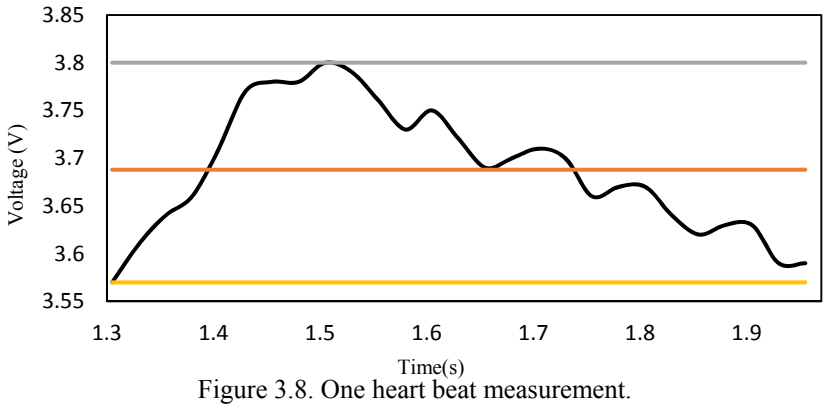

Figure 3.8. One heart beat measurement.

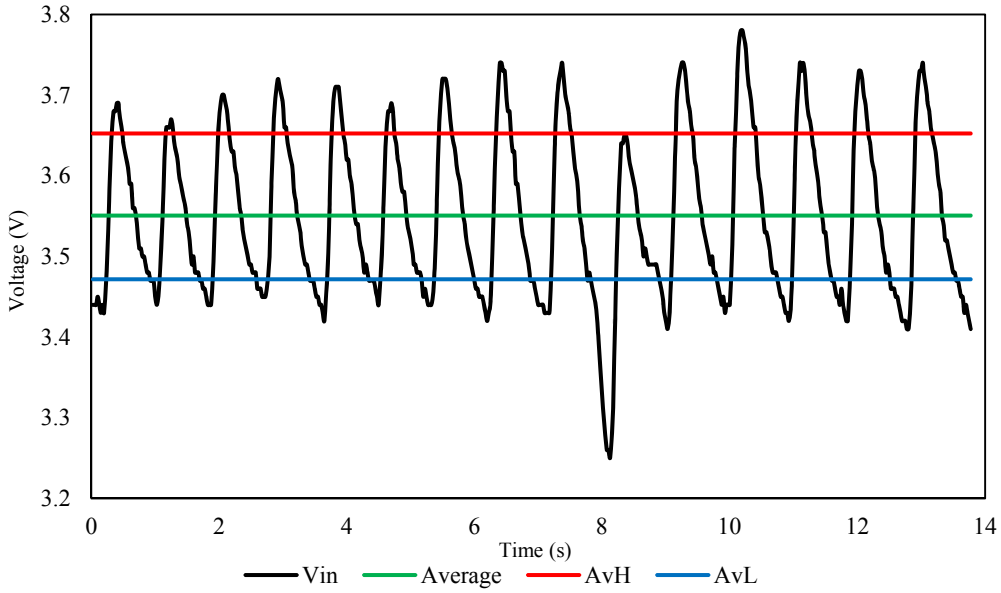

Figure 3.9. Another heart beat analysis from the Vin. Showing 15 beats in 14 seconds. A heart rate of 65BPM.

It is clear to see the heart rate from Figure 3.9 has a rate of 65BPM derived from the reading of 15 beats in 14 seconds.

Whilst this can be manually determined, the Arduino can be programmed to understand the definition of what a ‘heart beat’ is using only the Vin and time. This can be achieved by finding the average (green line) of 3.55V. Every time the Vin is above 3.55V, a counter can take note. There are ~16 voltage readings above this threshold within every heartbeat. There are a total of 241 reading above the 3.55 threshold within 13.775s. Taking the total instances of voltages above the threshold by the amount of voltages per heartbeat will give us the amount of beats within the reading; (241/16 = 15). As we can see and prove there are 15 beats within the 13.775

seconds leading to a heartrate of 65BPM ((15/13.775)/60). Now it is possible to mathematically calculate the heartrate with use of Excel, we now can move onto programming the microcontroller to tell it when to produce a beat against a timer.

The pulse can be programmed by telling the microcontroller that when the voltage reading is above the average reading, note a recording. As it is necessary to only note a pulse when the reading is above the average reading once, a counter can be implemented which can state that the value has to go down (below the average) before it can go up again.

Now the microcontroller can acknowledge a pulse, a timer can be implemented which will run against the counter. The microcontroller will read 30 pulses before the counter and timer is reset. A liquid crystal display (LCD) will display the results of the heart rate whenever the counter reaches the 30 beats. This is due to the possibility of null readings and ensures that faults within the reading can be reset.

The ring heart rate monitor can be placed comfortably on the finger. If the heart rate is too high or too low, the micro-controller can send a message via Bluetooth, internet or radio frequency (RF) and so alerting any nominated medical professional(s) to the readings. The circuit has very little technology associated with it and is very affordable but produces a gateway for medical carers to know how their patients are getting on. The programming code for the heart rate monitor is shown in Chapter ten, Appendix 10.1.

3.4 Heart Rate Conclusion

This chapter has discussed and produced a heart rate monitor using photoplethysmography's transmissive mode.

Being able to deduce the heart rate continuously whilst the user is comfortable and able to continue with their daily habits will enable a general picture of the user's heart rate activity and record how the user's heart rate acts during exercise and rest.

If the user is exercising, a target heart rate will be set allowing the user to maintain optimum levels for effective exercise. As an aside, by combining this data with data from others using similar devices, we can eventually build up a picture of the

average heart rate for any individual in comparison with others of their sex, age and weight. This might allow the user to be ‘rated’ against others and allow the competitive element present in many to spur themselves onto greater fitness.

During sleep, the heartrate is much slower. If the heartrate is seen to increase in combination with readings from the ring SpO2 monitor (discussed in chapter 5) decreasing, the device would recognise sleep apnoea and alert the user, a health professional or a further appropriate device. Monitoring the heart rate on a continuous basis will allow the device to inform the user if they are becoming unwell with an irregular heart beat or could help alert them to possible early signs of heart disease.

Chapter 4

4.0 Body Temperature

Body temperature is another vital that is commonly used when diagnosing a patient's illness. This chapter will discuss and implement an existing temperature sensor to find the body temperature of the user which it is aimed to incorporate into the ring device.

4.1 Body Temperature Introduction

Enabling a medical practitioner to know the temperature of their patient is very important. The hypothalamus is the part of the human brain that controls the body temperature [14]. If the patient's body temperature is above the average 36.5˚C to 37.5˚C, they could have hyperthermia and if the patient's body temperature is below, they could have hypothermia. If a user monitors their temperature with a continuous thermometer device and the patient reports that they now have a high temperature, the medical examiner would be able to review their historic and usual temperature to see how this compares with the instant readings and whether there is any observable pattern. If continuously monitored after a fever has been noted, any improvement can also be tracked.

The LM35 transistor works by collecting an analogue read from 0 to 1023. This figure is created by the change in voltage across the sensor which is directly proportional to the change in temperature [15]. As the output value can change with every measurement, it is appropriate to take an average of the analogue number read by the micro controller.

4.2 Body Temperature Background Research

Measuring body temperature is very important for patient diagnosis. The University of Illinois has devised a body temperature sensor that is only 50 microns wide and is placed on the wrist [16]. The flexible sensor can measure body temperature to thousandths of degrees. It is primarily made of gold and silicon. It is clearly a very innovative way of measuring body temperature but seems to be almost invasive as the report states *'bonding to the body almost like a second skin'*.

To avoid such invasiveness, the proposed body temperature sensor will be placed within the ring with the sensing node on the inside of the ring. There are a couple of rings that are able to measure temperature [17] but they all seem to measure it chemically and thus no batteries are required. Whilst this is potentially helpful so far as any requirement to power the device, as there are no electronic sensors involved and so there is no way of automatically logging the temperature of a user throughout the day.

4.3 Room Temperature Testing

As the baseline temperature reading of the device has to be as close to room temperature as possible, the LM35 transistor must be kept away from any other electronic devices such as any computer, and any other stimuli that may give off heat. A digital room temperature sensor was used and the sensor has to be as physically close to the room temperature sensor as possible, as shown in Figure 4.1.

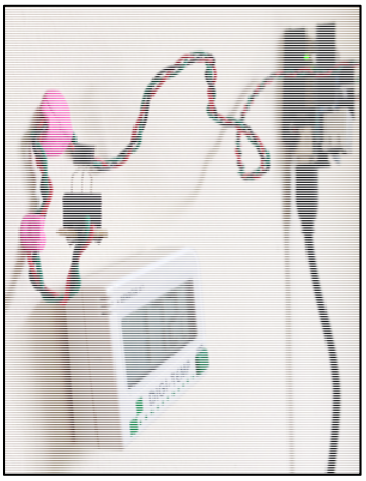

Figure 4.1 Room temperature digital device with the LM35 transistor placed on the wall.

The value of the sensor was recorded every 15 seconds for one hour with the room temperature ranging from 17.5 degrees to 18.9 degrees. When the data was collected, the values were averaged at the given temperature. The results showed that the readings were accurate and it would be possible to try to calibrate the sensor appropriately for human skin.

4.4 Body Temperature Implementation

The LM35 transistor could be placed within an elasticated ring in a similar manner to the heart rate monitor proposed above. A bracelet was made to obtain a

temperature reading more quickly and for convenience, given the ambit of this thesis, as the LM35 transistor available proved difficult to hold in place on the finger without any further development.

As the voltage is proportional to the analogue feedback from the transistor, it is simple to convert to the corresponding temperature. As the maximum analogue reading is 1023, this can be converted to a maximum temperature of 50˚C. The average body temperature is between 36.5˚C and 37.5˚C, so the LM35 transistor has a suitable range.

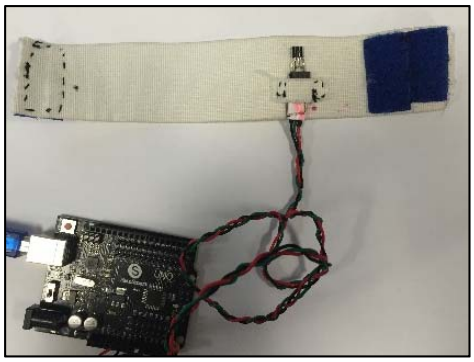

Figure 4.2 shows the temperature sensor in the elasticated material with Velcro on the ends to easily strap it to the wrist.

The temperature sensor records a reading every second and adds the reading to a running average over the last minute [18]. This prevents null results and keeps the temperature reading of the body temperature within a compliance of 0.4˚C accuracy.

The temperature sensor has to be calibrated to the body. Measurements were taken where the real temperature was recorded with a digital clinical thermometer as a benchmark alongside the temperature recorded by the sensor. After taking measurements as body temperature changed, the sensor could be calibrated.

Real Body Temperature (˚C)	Sensor Reading (˚C)
36.9	33.2
36.7	32.2
36.6	31.7
36.5	31.3

Table 4.1 shows the correlation found between real body temperature and the sensor reading

Using the fact that 0.1˚C of change in temperature produced a change of 0.49V from the sensor, it was simple to add more values to the readings. A graph (as shown below; Figure 4.3) was plotted where the use of the formula;

$$Y = MX + C \qquad (4.1)$$

Where Y is the real temperature, M, the gradient, X, the sensor reading and C being the Y intercept.

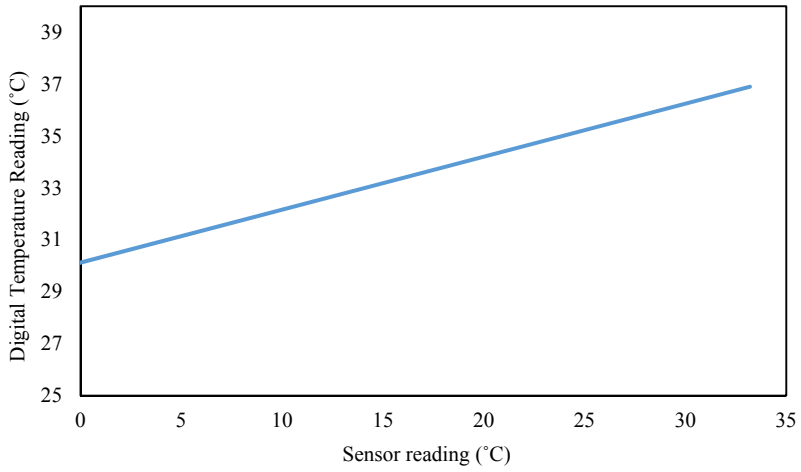

Figure 4.3. A graph of the digital temperature readings against the sensor reading.

To find the gradient, M, The formula; $M = \frac{\Delta Y}{\Delta X}$ (4.2) can be used where the change in Y = 0.9 and the change in X is 4.4 giving a gradient of 0.2045. The Y intercept

can be found on the graph and produced a value of 30.105. Consequently, the real temperature can be found when inserted into the formula:

$$Y = \left(\left(\frac{\Delta Y}{\Delta X} \right) X \right) + C \qquad (4.3)$$

Thus, if the reading from the sensor is 31.25, the real temperature of the body is ~ 36.5˚C. This reading takes into consideration the elastic material and any increased heat produced between the elastic material and the skin.

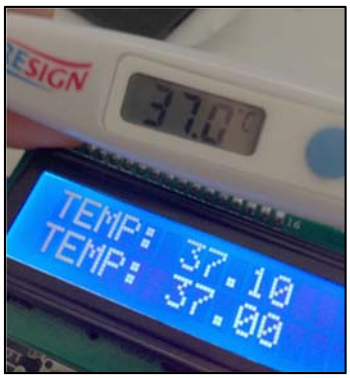

Figure 4.4. A photo of the digital thermometer next to the LCD screen's predicted temperature.

Figure 4.4 shows a photograph of the temperature sensor's reading printed out on an LCD screen next to the reading on the digital thermometer. The code for the temperature sensor is found in Chapter ten, appendix 10.2.

4.4 Body Temperature Summary

This chapter has discussed and programmed an LM35 transistor to measure the temperature of the body. Although it is currently cased within a bracelet and not a ring device, with further design and development this could be placed within a ring and recalibrated by using the same technique. The temperature could be made into the ring and send the corresponding body temperature to a base station that would record the value and produce a stimulus such as inform a medical examiner if the values are not at the average level for the specific user. The temperature sensor could be integrated with the heart rate monitor and the SpO2 device (produces in Chapter five) temperature device will be present when changes in temperature, heart rate and oxygen saturation levels if the user is unwell.

Chapter 5

5.0 SpO2

The oxygen saturation level within the blood is very important, known as one of the 'vitals', it is one of the standard measurements for health professionals. SaO2 is defined as the percentage of haemoglobin with bound oxygen and is termed as SpO2 when measured by a pulse oximeter. This chapter will discuss SpO2 monitors and implement a novel way of measuring the oxygen saturation of the user.

5.1 SpO2 Introduction.

In 1945, most deaths occurred in the home. By the 1980s, it was reduced to just 17% [19]. This statistic shows how far medicine has come on in just 60 years. People are living longer and have a better quality of life than at any other time in history. As we have better technology, we can detect health problems earlier than ever before and thus, we can take precautionary measures. Given that one of medicine's key aim is to pick up evidence of illnesses before symptoms occur [20], we can measure the key body symptom parameters of a human whose clinical condition is deteriorating within the home with help of wearable sensors [21] [22][23][24][25]. The average oxygen level is 95-100% [26]. An oxygen level below 90% is considered low, resulting in hypoxemia [26]. In this paper, we will discuss the measurement and monitoring of the SpO2 as one of the 'vitals' of the human body. We will also discuss another unconventional way of measuring SpO2 by utilising the wavelength of the oxygen-bound haemoglobin, to decipher the oxygen level. This technique is different from the methods used today. The proposed device is wireless, robust and will be implemented in the form of a ring to be worn on the finger, so the user may use the device at home without being disturbed by wires.

There are two types of haemoglobin; functional and non-functional. Functional haemoglobin binds and transports oxygen through the body and non-functional haemoglobin cannot bind or transport oxygen and is present as carboxyhaemoglobin (bound to carbon monoxide) and methaemoglobin which contains ferric iron (Fe3+) [27]. There are two types of functional haemoglobin;

oxyhaemoglobin (HbO2) and deoxyhaemoglobin (Hb) [27]. Body tissues absorb light differently which can be used to calculate the oxygen saturation of oxyhaemoglobin and deoxyhaemoglobin by using the formula [28]:

$$SpO2 = \frac{[HbO2]}{[HbO2]+[Hb]} \tag{5.1}$$

Using a pulse oximeter, a volumetric measurement can be obtained with aid of differences of light absorption within the blood, this method is known as photoplethysmography (PPG). As a SpO2 monitor needs to measure the percentage of haemoglobin with bound oxygen just within the arterial blood, a manipulation of taking the pulsatile flow and non-pulsatile flow can be used. The pulsatile flow is a measurement of the arterial blood, background tissue and venous blood. The non-pulsatile flow is the combination of the background tissue and the venous blood. Therefore, taking the non-pulsatile from the pulsatile flow will leave just the arterial blood value. The apparatus needed are two LEDs and a photo detector. The two LEDs are of different wavelength; 660nm, red light and 910nm, Infrared light (IR). Oxyhaemoglobin partially absorbs the IR light and deoxyhaemoglobin absorbs red light. The processor can then calculate the concentration of deoxyhaemoglobin and oxyhaemoglobin. A graph of the absorption of Hb and HbO2 can be seen in figure 5.1 below [29].

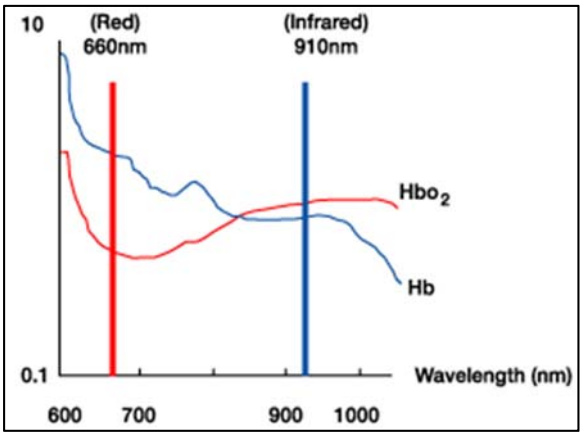

Figure 5.1. A graph of the absorption levels of haemoglobin and Oxyhaemoglobin. Haemoglobin. Haemoglobin absorbs light best art 660nm and Oxyhaemoglobin absorbs light best at 910nm.

The stated formula (5.1) can be used to determine the overall percentage of the oxyhaemoglobin within the arterial blood. The most common places for a SpO2 monitor to be attached to are finger, toe, or ear. These measurements give an accurate reading although can be misread if the user is wearing red finger nail varnish or if the monitor is moved and the processor calculates absorbed light wrongly.

Should oxygen saturation level fall below 90%, hypoxemia occurs. Causes can be (inter alia) sleep apnoea, asthma crisis or pulmonary infection [26]. A. Nobuyuki *et al* [30] perform an experiment which monitors a patient with sleep apnoea and measures their snoring with sound measurement and SpO2 values. The measurements were obtained at their home to aid a restful night's sleep as it was deemed unnecessary for the patient to be in the hospital for the trial measurement. The patient had a pocket sized SpO2 monitor on their finger. Although the WEC-7 SpO2 monitor was small and unobtrusive, the patient still had to sleep with it on the finger. This could have led to a disturbed sleep for the patient and so the results would not show a typical night's sleep. The experiment would have also been disrupted if the measurements of the levels were erroneous if, for example, the patient rolled over or let some external light through the monitor during REM sleep. If the patient had been wearing a different or less intrusive SpO2 monitor, they might have had a better night's sleep and the researcher may have obtained more reliable and consistent results without the threat of the SpO2 monitor potentially falling off. Some SpO2 monitors may be able to read the SpO2 over a period of a day but it would be much harder to gain the results over a longer period of time with a SpO2 monitor on an extremity [31].

Wearable sensors can be placed on many places of the body in contemporary wearable sensors including; stick-on electronic tattoos or directly printed onto human skin to enable long-term health monitoring [32]. As the sensor technology is improving so vastly, it seems appropriate to produce a sensor that is comfortable and convenient for the user. Many individuals wear rings as jewellery and do not remove them at night and so are conditioned to wearing them.

As the traditional SpO2 monitor needs to be attached to a bodily extremity to work, it would be difficult to monitor the oxygen saturation during the whole day. In this research paper, we explain a unique way of measuring SpO2 by using the colour of the blood and not the absorption difference of oxyhaemoglobin and deoxyhaemoglobin. This method is produced as a ring and not an extremity device for easier use within the home mainly due to the purpose of a user being able to use their fingers if the device was as a ring and not on the end of the finger.

There are few sensor artefacts that have been the subject of publication (but which are not yet commercially available) regarding ringed devices though use the traditional absorption method to calculate the oxygen levels. J. Sola *et al* [33] show the ring attached to the left index finger. The ring sensor is worn on the left hand and the calibration SpO2 monitors are worn on the right. The SpO2 around the whole body varies as there are more/less capillaries and different blood flows depending on parts of the body that need more oxygen than others. It is difficult to say even that the SpO2 level is the same for both hands at any one time if they are any great distance apart. Another known prototype of a ringed SpO2 monitor is produced by F. Adochiei *et al.* [34], the device transmits the SpO2 and heart rate value via RF to a patient monitoring device which logs the data received. The monitor, like J. Sola's monitor also uses the absorption method. Choosing the correct material for the sensor is also very important as it must not interfere with the monitoring readings. There are technologies available now that allow sensors to be woven into materials ready for detection. Plastic optical fibres (POF) can be used to measure SpO2 with help from 690nm and 830nm lasers [35]. These fibres can be very expensive for the final product which needs to be robust and sustainable to be worn over long periods of time and in case of medical institutions, used on different patients.

There are also few health monitoring sensors that measure other vitals via the use of a ring [36]. Considering most health problems within the home occur in elderly patients, it is important to keep the technology simple and easy to use; the less interaction the users have with the monitoring devices, the better. There are technologies around that permit the user to view their health vitals in real time via

use of a smart phone [37]. As there is currently no available technology that will allow a continuous SpO2 monitoring within the home, a system needs to be implemented which can measure SpO2 and send it on to a medical examiner to view the patients history of oxygen saturation during the day and night.

In this research paper we intend to demonstrate a correlation between the wavelength of the oxygen bound haemoglobin and the percentage of oxygen bound with haemoglobin. The higher the wavelength: the higher the SpO2 value. We show that the proposed optical sensor is able to detect a change in oxygen saturation via the colour of the blood. The more oxygen within the blood, the brighter the red; the brighter the red, the lower the red value of our proposed colour sensor will be. We report a unique SpO2 monitoring optical sensor device which is affordable as the sensor used is quite basic and already pre-embedded making it compact and robust. The user will be able to comfortably use it all day/night, performing real-time measurements, without any uncomfortable irritants.

5.2 Spectroscope measurement of SpO2

The unconventional method proposal statement is as follows: Blood is red because of the protein ‘haemoglobin’. Haemoglobin has a molecule called a "heme" which has the metal iron in it. When the iron is oxygenated, it becomes red. When the iron is deoxygenated, it becomes a darker red [38]. Using this statement, the prediction can be made that the more oxygen the blood has, the brighter the red will be, therefore, a longer wavelength should be produced. Likewise, the less oxygen there is within the blood, the shorter the wavelength should be.

An experiment was set up to see the correlation between the wavelength of the haemoglobin within the blood and the SpO2 value. A high intensity white LED was placed on the nail side of the index finger and a spectrometer (on the opposite side) was recording the wavelength in the blood. At the same time, a SpO2 monitor was placed on the middle finger. When the output of the spectrometer was saved, the SpO2 reading was recorded. Figure 5.2 shows the schematic of the spectrometer set up of the index finger's system. An ultra-bright LED is used to ensure maximum penetration through the finger. It must be white light so that all of the wavelengths are emitted, this is crucial in discovering the SpO2 as the wavelength absorbed by the blood can be found. The index finger is used as the SpO2 monitor is more comfortable on the middle finger to help the experiment run smoother and obtain quicker and accurate results. After the LED is shone on the nail side of the finger, the spectrometer can be used to find the wavelength of the oxygenated blood. The spectrometer's sensor is attached to an optical fibre to gain the fastest result to be read. Once the spectrometer has saved the wavelength, the SpO2 value is noted for use later.

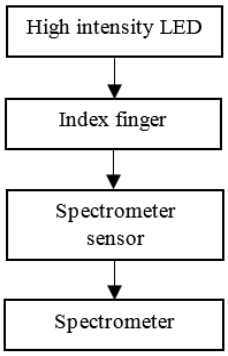

Figure 5.2. Schematic of the spectrometer set up.

Figure 5.3 shows the measurement being taken with the spectrometer's sensor with the index finger and the SpO2 monitor on the middle finger. There were two people participating in obtaining the results. During the experiment, the room's lights were turned off and the spectrometer's sensing cable was placed firmly on the finger to reduce the ambient light reach the sensor.

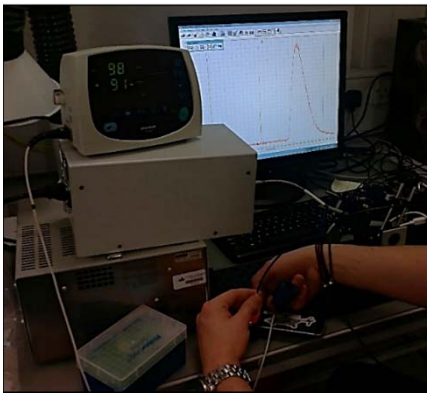

Figure 5.3.Photograph of the spectrometer measurement attached to the index finger with a phone's bright LED on the nail side and the SpO2 monitor attached to the middle finger.

5.3 Spectrometer measurements, results and discussions

The results were obtained after the spectrometer completed the readings of intensity of transmission at different wavelengths. Each reading number was noted next to the respective SpO2 value. The results suggested a correlation between the higher the oxygen levels, the higher the peak wavelength. Figure 5.4 shows the spectrometer reading when the blood oxygen was at 97% for person 1, the peak wavelength is at 632 nm. The x-axis represents the wavelength measured in nm and the y-axis is the intensity level that can be changed by the colour of the skin, thickness of the finger and the amount of light received by the spectrometer. The intensity's units are watts per square meter, so a slight change in position of the spectrometer's placement on the finger could result in a large change in intensity. A peak can be seen between 430nm and 450nm within many of figures. This peak is within the ultraviolet spectrum. Although its intensity reaches up to ~40% of the peak wavelength at 632nm, it can still be seen as insignificant as it is only the red wavelengths of values 620nm to 750nm which are being monitored as W. Nahm *et al.* [39] shows the changes in tissue absorbance caused by blood pulsation. The non-invasive experiment showed a different relation between absorption at 600 and 910nm. As this is within the red spectrum, we can look specifically within this range.

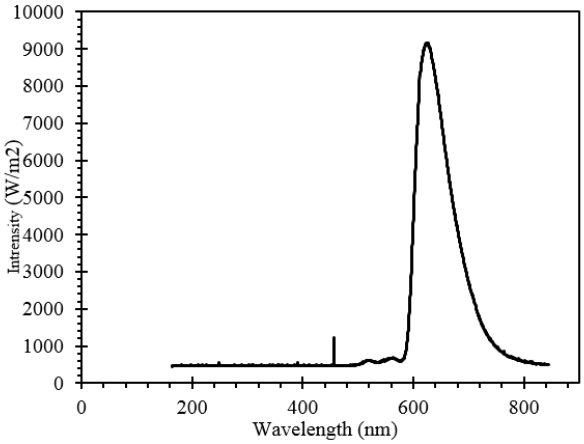

Figure 5.4. Graph of the first participants' wavelength when the SpO2 level was at 97% with the peak wavelength at 632nm. Values below 600nm can be ignored as only the red light wavelengths are relevant for measuring pulsative blood need detection.

Figure 5.5. Shows the spectrometer's reading when the SpO2 value was at 96% for person 2. The peak wavelength is 624 nm. Figure 5.5.a illustrates both participant's results together in one graph. The oxygen levels were both at 97% and the peak wavelength of each person's result was 632 nm.

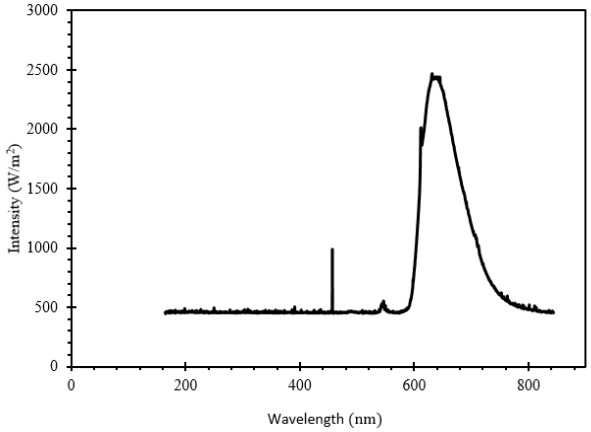

Figure 5.5. Graph of the second participant's wavelength when their SpO2 level is at 96%. The sharp peak at 624nm suggests a lower SpO2.

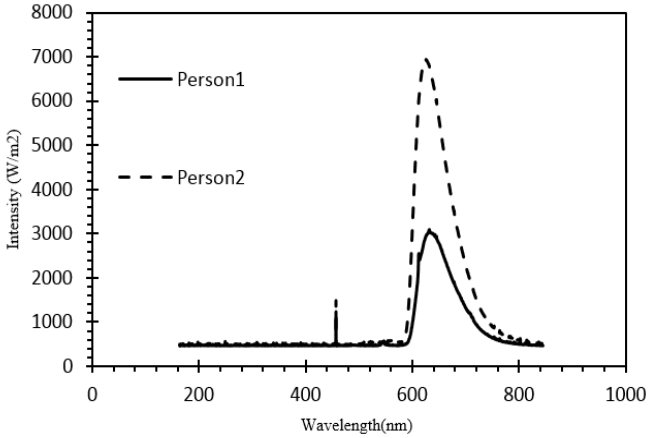

Figure 5.6.a. Graph showing the first and second participant's wavelength when both participant's SpO2 levels were at 97%. They both have the same wavelength peak but a different intensity level.

It is clear to see that the second participant's y-axis value of intensity is much higher than the value of the first participant. This could be caused by the difference in fingers of the participants. Skin colour, thickness, light received to the spectrometer and other variables will change the intensity. This is not a problem as it does not affect the wavelength of the result. Therefore a person's skin tone or difference in thickness of fingers for said person does not affect the overall result.

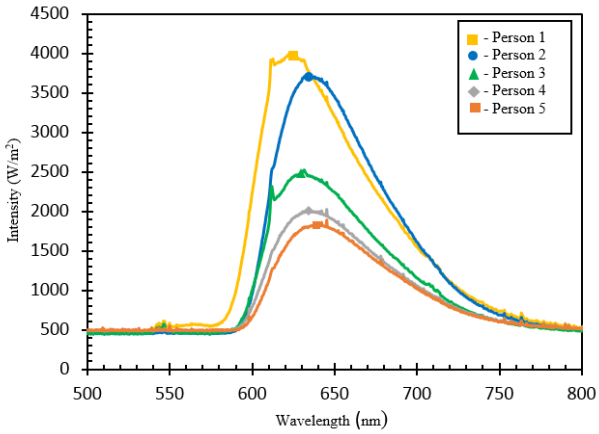

Figure 5.6.b. Graph showing five different spectrometer readings with different participants. Each participant has a difference in intensity and wavelength.

Figure 5.6.b shows five different SpO2 readings from the spectrometer. It is clear to see the shift in wavelengths shows that the red colour of the blood is a different shade of red. This clearly shows that as there are different colours of red within the blood, the oxygen binding is different in each reading. The yellow line (person 1) has a wavelength of six hundred and twenty six nanometres, the blue line (person

2, with the highest wavelength) shows six hundred and forty two nanometres, the green line (person 3) has a wavelength of six hundred and thirty three nanometres, the grey (person 4) at six hundred and thirty seven nanometres 637nm and the orange (person 5) is at six hundred and forty nanometres.

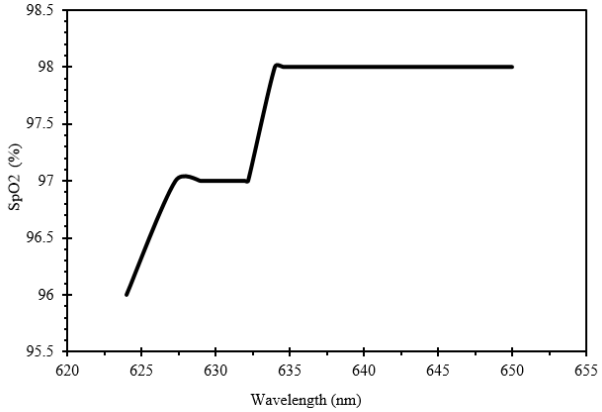

Figure 5.7. Graph showing the change in wavelength over level of SpO2. The higher the peak wavelength, the higher the SpO2 value.

Figure 5.7 shows the overall results from the peak wavelengths and their corresponding SpO2 Values. It shows that the higher the wavelength, the higher the SpO2 value. The spectrometer used within the experiment was a Hamamatsu mini spectrometer, a highly sophisticated and accurate device. When the SpO2 is at 98%, the highest recorded value was 650nm and the lowest at 634nm. The range of SpO2 at 98% is 16nm. When the SpO2 value is at 97%, the highest value given is 632.2nm and the lowest 627.3nm, giving a range of only 5nm. As only one 96% value was recorded and the spectrometer saves the value over a duration of about 10 seconds, the real value may have been just a low 97% and thus the range could be at least 10nm, which is more likely. Never the less, it is clear to see that the higher the wavelength, the greater the value of SpO2.

As this experiment indicated some evidence of correlation with respect to the prediction, it can now be taken to the next stage of creating the sensor at a much lower price without affecting the accuracy. We developed a home-made spectrometer using black card. A slit can be inserted into the bottom to let the light in and then a sheet from a DVD-R can be used for the diffraction grating to reflect the incoming light from the slit onto the bottom of the card [40]. The card spectrometer was made into a strengthened black plastic model by using the same dimensions within the 3D printer shown in Figure 5.8. The model is extremely affordable to make as it is made up of a small amount of plastic and a DVD. This can then be placed onto a digital camera to take a photo of the given spectrum shown in Figure 5.9.

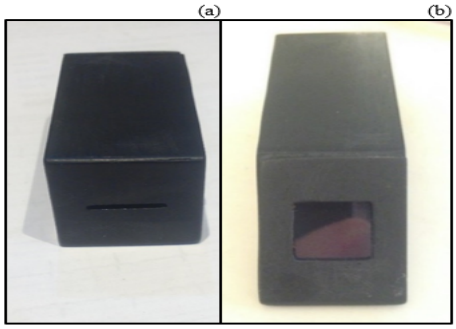

Figure 5.8.a Back view of 3D printed spectrograph with slit (15mm x 2.5mm). 5.7.b Front view of spectrograph with diffracting grating (15mm x 15mm).

Figure 5.9. Image of 10.1 MP camera attached to the spectrograph. The diffracted light entering the slit can be captured.

The 10.1 MP camera captured white light via the 3D printed spectrometer, with the output shown in Figure 5.10 (a), displaying the whole visible spectrum. Once the 3D printed spectrometer was attached to the camera lens, a finger can block the slit with a high intensity LED behind the finger to allow the camera to view the absorption of the finger. The red light is passed through and the colour of the blood can be captured as seen in Figure 5.10 (b). The next step is to deduce the peak wavelength of the new red image.

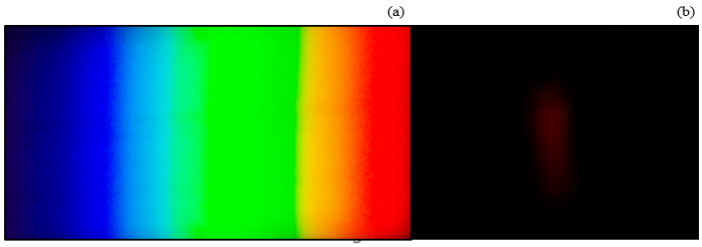

Figure 5.10. (a) An image captured by the camera of white light through the slit. It shows the visible spectrum. (b) An image of the index finger's blood colour. The image's colour can be analysed to work out its corresponding wavelength and thus SpO2 value at that moment in time.

Processing the image's wavelength of the colour red produced and captured will help to measure the SpO2. MATLAB could be utilised to turn the image into greyscale and calculate the amount of colour within each pixel. These values could then be plotted against the wavelength of known pixels of laser light to calibrate the MATLAB program. We deemed it unnecessary to produce said program as the spectrometers' main job was to produce the proof of concept. As there is a noticeable correlation between the wavelength and SpO2, we can begin to investigate further. As the spectrometer is very expensive and difficult to fit into a ringed device, it seemed appropriate to implement a device that can view the change of wavelength.

5.4.0 Measuring SpO2 with a TCS3200 colour sensor

Another experiment is set up where a TCS3200 colour sensor measured the amount of redness within the blood. The said sensor had a bright LED attached to it which is always on whilst the sensor is recording. The TCS3200 was deemed the best sensor to use as it already has an ultra-bright LED in a fixed position and brightness to which will eliminate any intensity problems we may face. The TCS3200 is considerably affordable and produces very accurate results. The microcontroller

used was an Arduino Uno. The Arduino was programmed to take a reading of the colour sensor's red, blue and green values. The experiment only took account of the red values from the colour sensor every second which was then stored onto a secure digital (SD) card to later be evaluated. The new device was placed on the index finger of the right hand and the SpO2 monitor was placed on the right hand's middle finger to keep the variables constant for later correlation use with the first experiment. A counter was programmed to view which value corresponded to each measurement, when the SpO2 value changed, the counter's number was noted.

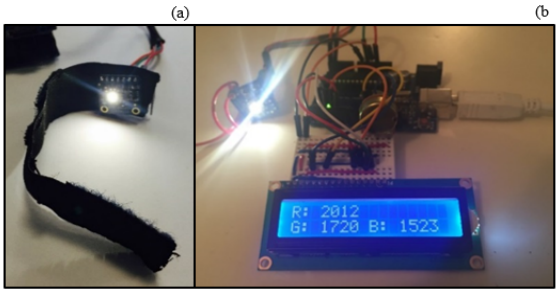

Figure 5.11. (a) A photograph of the colour sensor attached to the elastic for the ring. (b) Shows the colour sensor attached to the Arduino Uno. After the red value has been found, it is printed onto an LCD screen and updated every second.

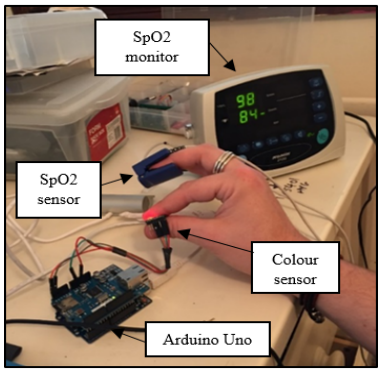

Figure 5.12. Shows the index finger holding the colour sensor with the bright LED being fed to the Arduino micro controller to store the data and the SpO2 sensor attached to the middle finger being read by the SpO2 monitor.

5.4.1 Ring device results

The results obtained by the colour sensor showed that as SpO2 increased, the red value decreased. As the sensor worked by using the intensity and the colour, the colour of the skin, thickness of the finger and finger placement affected the red's value, therefore the red value would be different for every user, although it did not change the fact that the redness of the blood was inversely proportional to the blood's oxygen saturation. The red value measures the saturation irradiance and gives a unit of µW/cm2 [41]. As the intensity of transmitted light is low passing through the finger, the sensor will produce a high value. The higher the red value, the more red the entity in front of the sensor is.

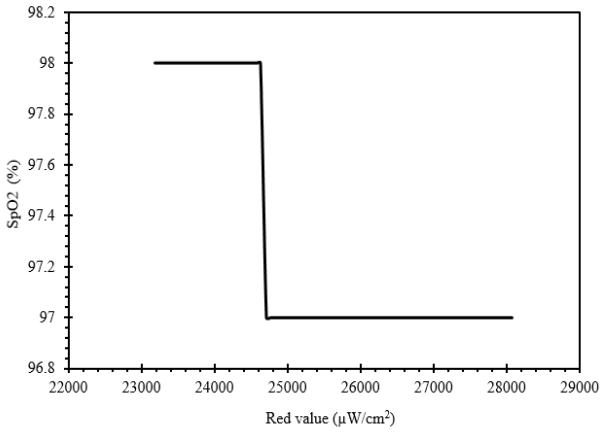

Figure 5.13. A graph of the change in Red value as oxygen levels changed. It shows the higher the red value, the lower the SpO2.

The obtained results in Figure 5.13 from one of the tests shows that as the red value increases, SpO2 decreases. As only two values of the finger's oxygen saturation were taken, it is difficult to deduce the range of each value's average value of the SpO2. Furthermore, we conducted another test where all of the corresponding red values to SpO2 are averaged out to view how the values are affected (shown in Figure 5.14.a).The results concluded that the values obtained decreased proportionally. If more values for the 95% SpO2 values were recorded made at a lower decimal, the red value would have been higher and thus produce a more inversely proportional graph. This makes sense as the more oxygen within the blood, the more orange the blood is thus the levels should be lower. If the blood has less oxygen, it is a darker red, therefore the red value will increase towards the IR spectrum.

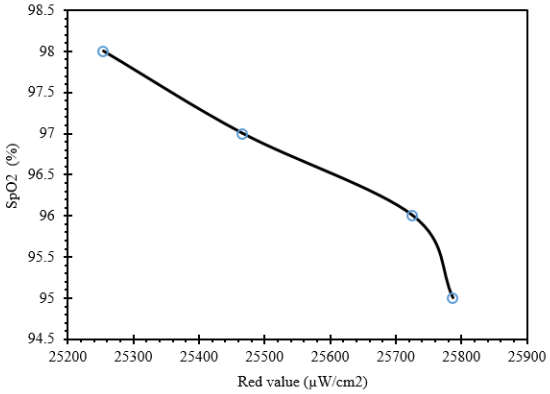

Figure 5.14.a. A graph representing the average SpO2's corresponding red value. As the red value increases, the SpO2 decreases proportionally.

Another participant's results were measured and showed that there was a range of about 700µW/cm^2 for every 1% change in SpO2. These results could be coded to produce the specific ranges in oxygen saturation for this particular participant. Each participant's red values were different as their fingers may have has a different impact on the colour sensor. Once recorded, each participant's individual range could be added to their sensor to allow their specific SpO2 value. Figure 5.14b. shows the participant's change in red value as SpO2 changed. The values ranged from 99% to 95% with a red value range from 20700 to 23450 µW/cm2. This gave a 1% change in SpO2 of ~540µW/cm^2 red value per known ranged values. Although the SpO2 monitor has not reached levels lower than 95%, it is possible to predict that as there is less haemoglobin with bound oxygen within the blood, the red value will continue to increase and will be able to predict levels lower than that of the said graph.

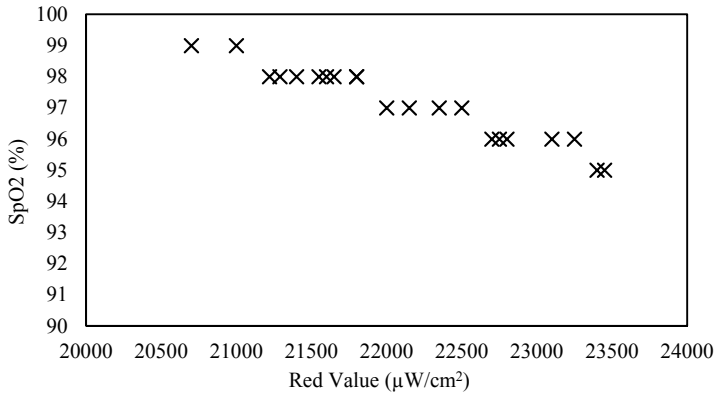

Figure 5.14b. A graph of a participant's SpO2 values ranging from 99% to 95% in SpO2 and 20700 to 23450 in red value. The graph shows that each value of SpO2 has a range of ~540µW/cm^2.

Taking the values from Figure 5.14b, we can use Pearson's product moment correlation coefficient to view the negative linear correlation [42]. The resulting value *r* should produce a value between -1 to 1. The closer the value is to 1, the more linear the correlation and the closer the value *r* is to -, the more linear negative correlation. A resulting value of 0 shows no correlation between the data. By taking the Y values (SpO2) and the X values (red value), we can insert them into the main formula:

$$r = \frac{Sxy}{\sqrt{Sxx \times Syy}} \tag{5.2}$$

$$Sxy = \Sigma xy - \frac{\Sigma x \Sigma y}{n}, Sxx = \Sigma x^2 - \frac{(\Sigma x^2)}{n} \quad Syy = \Sigma y - \frac{(\Sigma y^2)}{n} \tag{5.3}$$

Where Σx is the sum of all of the red values, Σy is the sum of all of the SpO2 values, Σx^2 is the sum of all of the red values squared, Σy^2 is the sum of all of the SpO2 values squared, Σxy is the sum of all of the red values multiplied by the SpO2 values and *n* is the total number of variables.

Table 5.1 below shows the values of *X, Y, X2, Y2,* and *XY* values used for the formulas and Table 5.2 shows the sum products; Σx, Σy, Σx^2, Σy^2, Σxy and *n*.

X	Y	X^2	Y^2	XY
20700	99	428490000	9801	2049300
21000	99	441000000	9801	2079000
21220	98	450288400	9604	2079560
21290	98	453264100	9604	2086420
21650	98	468722500	9604	2121700
21550	98	464402500	9604	2111900
21600	98	466560000	9604	2116800
21400	98	457960000	9604	2097200
21800	98	475240000	9604	2136400
21800	98	475240000	9604	2136400
22000	97	484000000	9409	2134000
22150	97	490622500	9409	2148550
22350	97	499522500	9409	2167950
22500	97	506250000	9409	2182500
22700	96	515290000	9216	2179200
22800	96	519840000	9216	2188800
22750	96	517562500	9216	2184000
23100	96	533610000	9216	2217600
23250	96	540562500	9216	2232000
23450	95	549902500	9025	2227750
23400	95	547560000	9025	2223000

Table 5.1. The X (red value) and Y (benchmark SpO2 value) values used to work out the product moment correlation coefficient.

ΣX	ΣY	ΣX^2	ΣY^2	ΣXY	n
464460	2040	10285890000	198200	45100030	21

Table 5.2. The sum products and *n* used for the formulas.

The results showed Sxy to be -18940, Sxx to be 13361800 and Syy to be 28.57. Once placed into the formula (5.2), the coefficient's value is -0.97. This shows extreme linear negative correlation between the red value and the SpO2.

Once the data values had been collected after many tests, the rate of change of SpO2 with the red value can be predicted and the SpO2 will be able to be worked out by using the red values with respect to themselves. Each user will have their own set of values that will need to be originally calibrated with the use of a SpO2 monitor as the thickness of fingers and colour of the skin can have an effect on the red value. After the calibration is completed, the SpO2 device is ready for use.

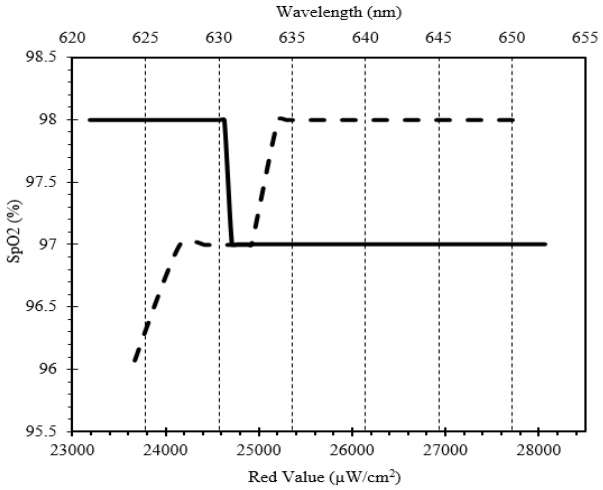

Figure 5.15. A graph representing the correlation between the wavelength and red value as SpO2 changed. As SpO2 increases, the red value decreases and the wavelength increases. This shows that the higher the red value, the lower the wavelength.

The above graph shows the obtained results of the spectrometer experiment and the Arduino's colour sensor's experiment. It shows that the higher the wavelength of the oxygen bound haemoglobin, the higher the SpO2. It also shows the lower the red value, the higher the SpO2. Our experiments demonstrate that there is a strong correlation between the wavelength and the red value of the colour sensor and can measure the wavelength of the oxygen bound haemoglobin. From this experiment, we can suggest the data implies a correlation between the wavelength of the oxygen bound haemoglobin and the change in oxygen saturation.

5.4.2 Making the SpO2 device wireless

The next step is to make the proposed SpO2 device wireless. We use 433MHz RF chips to transmit the red value to another device base. This way we save the energy on the data logging. As the antennas are of quarter λ and are 433MHz, it is possible to work out the optimum length of the antenna. Given that; $C = \lambda f$, where c is the

speed of light ($3x10^8$m/s), f is the frequency (433 x106Hz) and λ, the wavelength; we can calculate the optimum length of the antenna will be 0.693 meters. Due to the antenna being a quarter wave, the overall antenna length will be 0.173 meters (17.3cm). This can produce a radius range between the antennas at 30 meters. Though path loss is quite strong, at thirty meters, the power to receive the transmitted signal is still over the -105 dB limit. This shows that the signal can be received at the base device (which could be connected to the internet) in a large, thick walled house. Figure 5.16 shows the colour sensor, SD shield and transmitter device and another receiving device which can log the data.

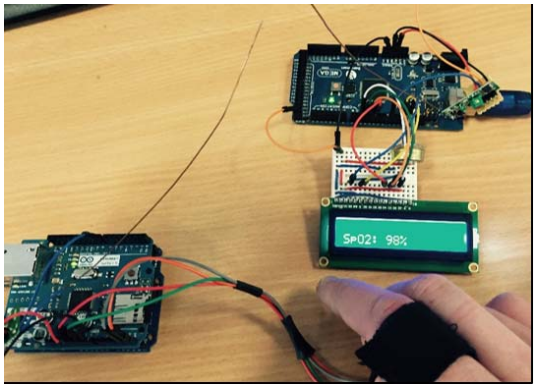

Figure 5.16. Left: Ringed device reading the SpO2 value and transmitting the value to the receiving device via a MX-FS-03V transmitter. Right: Receiving device displaying the SpO2 value via a MX-05V receiver.

The system results can now be interpreted by a mathematical model where each red value will be matched to a corresponding SpO2 value. A ring is made from black elastic material and the sensor is placed inside. Choosing the material for the proof of concept experiment was difficult as a material was needed for the ring to be comfortable for the user to wear over a long period of time. The black elasticated material assured that no ambient light or external factors affected the red value and also made the sensor exert the same pressure and maintain a fixed placement on the finger. Using the Arduino's serial monitor, the program is able to send the red value and the corresponding SpO2.

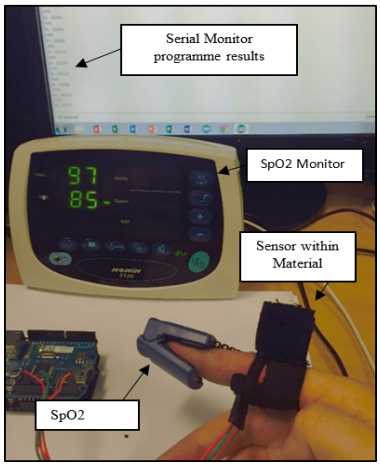

Figure 5.17. Shows a photograph of the accuracy testing with the SpO2 monitor and ringed device on the same finger. The serial monitor is reading the values from the program, ready to send to the server.

In our test experiment, we have involved three participants where the SpO2 monitor is placed on the middle finger and the ring is placed on the index finger in order to ensure an accurate reading. Every thirty seconds, the SpO2 monitor's value was recorded as well as the ring's SpO2 value. They were later placed onto graphs (Figure 5.19a/b/c) to see how accurate the ring was with the new method to the real oxygen value of the finger. The dotted lines are the real SpO2 values and the solid black lines are the device's calculation of the SpO2 by use of the red value.

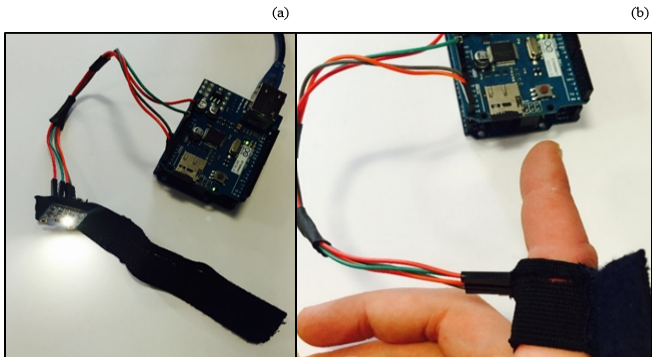

Figure 5.18. Two images of the ring device, (a) with the ring off and (b) with the ring on the index finger.

Our experiment results confirm that our proposed SpO2 monitoring finger ring is very accurate, it was never more than 1% out in absolute value. Five minutes is a sufficient amount of time to constantly check the monitor, to see when it changes as the SpO2 will fluctuate during said time. Though there was a slight lag in the device when the real value changed, after a couple of seconds, the device was able to stabilize to the correct value which shows a slight change in calibration is required. Person 1's results device value's highest SpO2 reading was at 98% and lowest at 95% (shown in Figure 5.19.a). The real readings for person 1's oxygen saturation levels read from 98-96%. Person 2's results fluxed between 99 and 98% (shown in Figure 5.19.b).When the values were off with the ring device, they were higher than the actual results which suggests the change in calibration could be to lower the red value ranges slightly. Person 3's device's results were only off once (shown in Figure 5.19.c). This was at the 1 minute stage where the real value was higher than the device's results by 1% at 98% and not 97%.

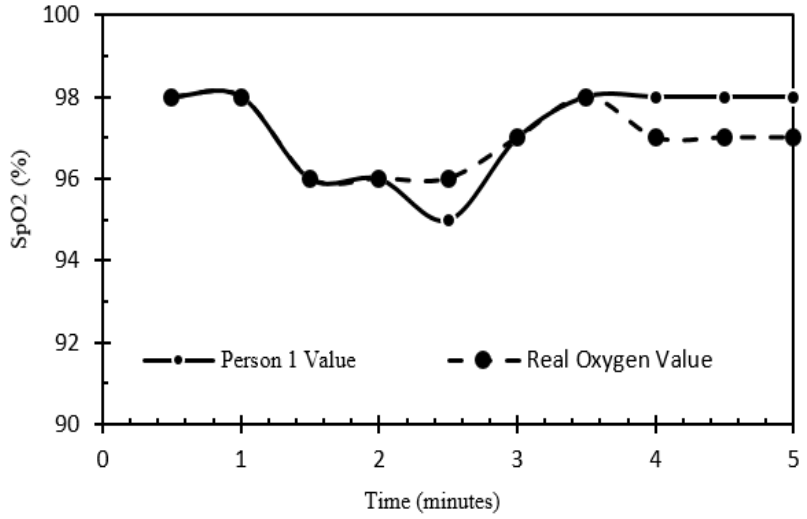

Figure 5.19.a. Person 1's accuracy testing. Absolute error no more than 1%. 60% matching with actual value.

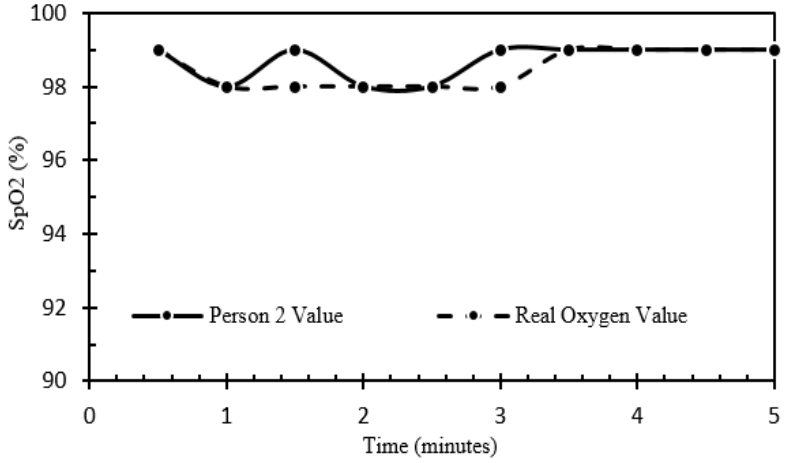

Figure 5.19.b. Person 2's accuracy testing. Absolute error no more than 1%. 90% matching with actual value.

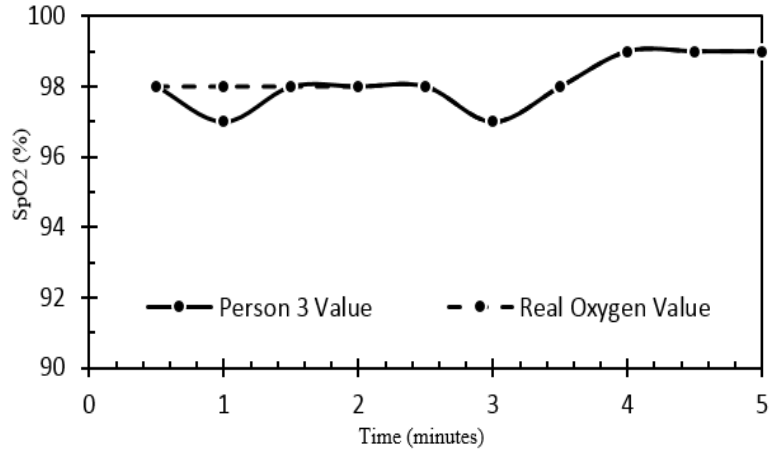

Figure 5.19.c. Person 3's accuracy testing. Absolute error no more than 1%. 80% matching with actual value.

5.5 SpO2 summary

We have demonstrated a SpO2 optical sensor monitoring device that would be able to be placed on the human body as a finger ring. We have developed the experiment and tested the proposed SpO2 optical sensor ring on real patients, where it has been shown to be accurate. The proposed SpO2 optical sensor ring is robust and easy to operate, which can be given to patients at home for maximum restfulness for the professional's assessment and save the use of hospital bed spaces. Our proposed and developed SpO2 optical sensor ring can be programmed to alert the user or health professional if the SpO2 level has fallen too much. It can also be programmed to see if the ring is being worn by the user.

Our proposed SpO2 optical sensor is a real-time device that can be worn on a daily

basis at home or outside of the home. A transceiver could replace the RF chips so that when the user is not at home, data can be logged onto the device and then sent to a base station. When in range again, RTS/CTS (ready to send/clear to send) protocol can be utilised. The SpO2 optical sensor will have a greater impact on users whose oxygen levels need to be monitored periodically or over a longer period of time. Costs will be low as the mathematical model within the microcontroller will enable just the one sensor to produce the SpO2 from the red value detected. This device can be easily integrated to other health vital measurements such as heart rate or body temperature.

Chapter 6

6.0 Blood Pressure

Blood pressure is a measurement of the arterial pressure within the blood vessels and can diagnose a patient's potential risks of problematic conditions such as a stroke, heart attack or an aneurism. This chapter will discuss blood pressure and introduce a potential method of estimating a user's blood pressure with use of the heart rate monitor proposed in Chapter three above.

6.1 Blood Pressure Introduction

A traditional method of measuring blood pressure is by using a sphygmomanometer. Usually used on the upper arm (concerning the brachial artery), the blood pressure can be deciphered by the user listening to the blood in the artery after being cut off. A standard reading for blood pressure is 120/80. The numerator is the systolic pressure, when the heart contracts and pushes the blood through the arteries. The denominator is the diastolic pressure, whilst the heart is relaxing and refilling with blood, thus the blood pressure could be seen as a range as it is constantly changing with every heartbeat.

A measurement can be taken by cutting off the blood in the artery for a short amount of time by inflating the cuff well above the average systolic pressure. When the cuff starts to deflate and allows the blood to rush through the artery again, the highest pressure can be established by listening to the blood 'spurting' back through the vessel during systole. When the noise stops, it means that the pressure has returned back to normal due to the blood coursing through the brachial artery again and therefore, the last sound heard can be deduced as the diastolic pressure.

The value of the blood pressure is an approximation and should it be done again for comparison and should be used on the same artery as the previous time as blood pressure can differentiate with different arteries, for example, the right brachial artery to the left. The blood pressure must be taken in a position where the arm is roughly equal to the level of the heart as if the arm is raised less pressure is forcing though the arteries due to gravity pulling it down and when the arm is lower than

the heart there is more pressure as the force of the blood through the arteries increases due to gravity and thus a higher blood pressure would be inaccurately recorded.

Blood pressure is currently rarely monitored on a continuous basis throughout the day, being mainly taken when a user goes to the doctor. Users have not felt the need to monitor their blood pressure in a similar way to the manner in which they have begun to monitor their own heart rate and have for many years have taken their own temperature when feeling unwell. Alas, this has led to a stagnation of innovation with the sphygmomanometer cuff method being the favoured but old fashioned technique. This might be worth reconsidering as users seek ever more accurate and complete information about their own vitals and health.

6.2 Blood Pressure Background Research

A new variation of the cuff method is a blood pressure dock, produced by iHealth [43]. A user's iPhone is plugged into a iHealth dock where a cuff is attached to it. The measurement is taken and sent to the phone's health app and costs around £55 ($80) The battery used is a 3.7V Li ion, the documentation for the device doesn't state battery life, but considering that it is a lower voltage than the operational voltage of 5V of the device, it is unlikely to be more than a couple of hours. This method can also be produced as a wireless wrist strap but still uses the uncomfortable inflatable cuff, this also costs £55 ($80). The only other apps concerning blood pressure have to be imported into the app by the user.

This proposal will set out a way to measure blood pressure without using the uncomfortable cuff method. A device has been designed by Massachusetts Institute of Technology (MIT) which uses a method called pulse wave velocity (PWV) [44]. PWV measures two points along the artery and utilises Newton's second law of motion (6.1).

$$F = ma \tag{6.1}$$

Where F is the force, m is the mass and a, the acceleration of the blood. The two points of the artery will be used to deduce the acceleration within the formula;

$a = \frac{v-u}{t}$. By using the formula; $P = \frac{F}{A}$, where P is pressure, F is force and A is the cross sectional area of the artery, we can obtain the equation:

$$P = \frac{(ma)}{A} \tag{6.2}$$

This will figure out the pressure of the arterial blood through the finger. The main issue with the proposed PWV method is that many assumptions must be made including that the area will always be the same. Assuming the device will be calibrated to the specific person of area of the artery is known, this will not enable the user to use the measurement on a different finger as the vessels and capillaries will be different throughout the body. If the method is used for a person still growing, the area will gradually change as their body gets bigger and thus will de-calibrate the individual.

Our proposed blood pressure sensor will not use the cuff method or the pulse wave velocity method and will cause no discomfort to the user. The paper will apply the PPG method, as used for the heart rate in Chapter four and photophelthysmography (PPG). Photoplethysmography is the technique of optically determining the blood volume changes. This sensor will use PPG to view the change in the output resistance of the heart rate monitor .This is a more innovative way and has, so far, only reached experiment stages but no further.

6.3 Blood Pressure Implementation

Md. Manirul Islam et al proposeds a non-invasive continuous blood pressure monitoring device with use of the photoplethysmography method [45]. The paper uses the similar method and theory of the proposed heart rate monitor within Chapter four. Using a high intensity LED and an LDR through the finger, blood pressure can be deduced after calibration. As the light is received through the LDR during systole, the LDR value is at a maximum and as the light is received through the LDR during diastole, the resistance is at a minimum. Thus, it is safe to assume that the resistance of the LDR is proportional to the blood pressure. Taking a view of the heart rate shown in Figure 6.1, produced by the device within the heart rate Chapter four, it can be seen that the theoretical systolic blood pressure (SBP) can

be calculated via the use of the maximum value of the heart rate (blue line on Figure 6.1) and the diastolic blood pressure (DBP) (grey line on Figure 6.1).

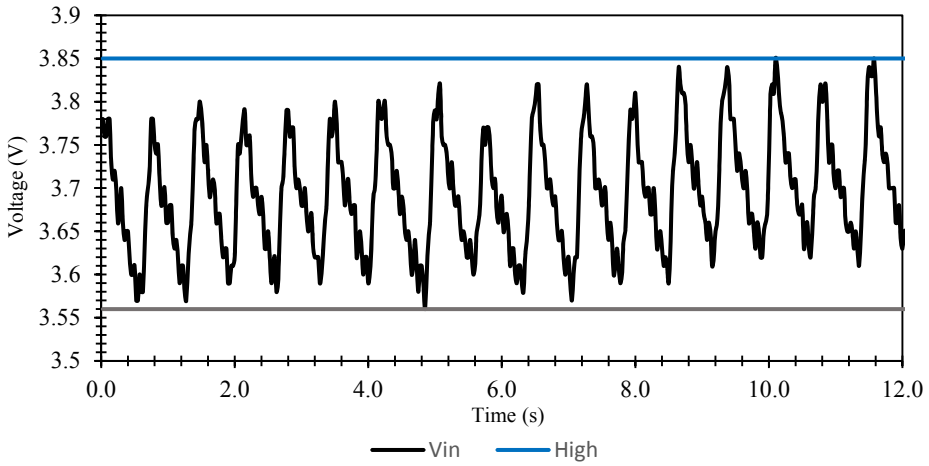

Figure 6.1. shows a graph of a heart rate measurement. The graph consists of 17 heart beats in 12 seconds; 85BPM.

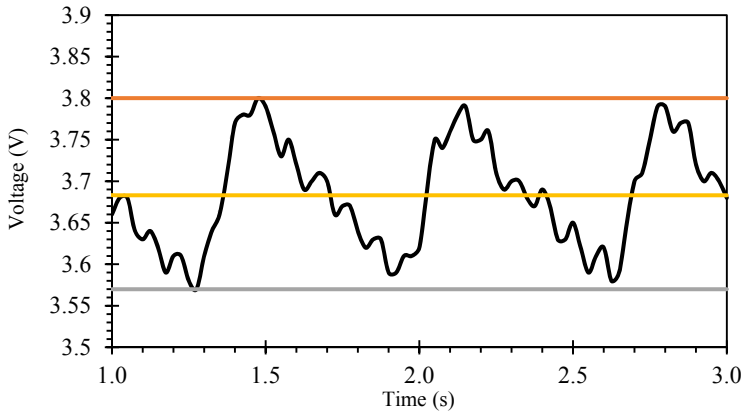

Figure 6.2.a. a portion of the heart rate graph from Figure 6.1.

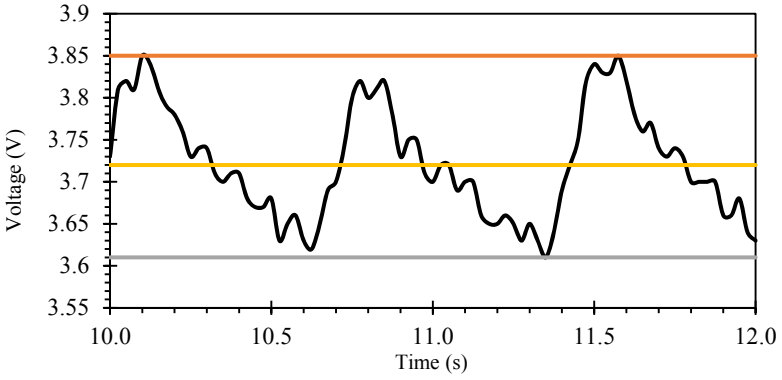

Figure 6 2.b. another portion of the heart rate graph from Figure 6.1.

Figure 6.2.a and Figure 6.2.b show the comparison of two separate heart rates. The

heart rate is easily deductible. Both Figures have about three heart beats in two seconds, making a heart rate of ~90 BPM. Figure 6.2.a has a maximum voltage of 3.8V and a minimum of 3.57V. Figure 6.2.b has a maximum voltage of 3.85V and a minimum voltage of 3.61V. As there is a higher voltage within the second, there is a higher resistance. As there is a higher resistance, less light is getting to the LDR compared to the first. As less light is getting to the LDR, there is a higher volume of blood within the finger. As there is a higher volume of blood, there is a higher blood pressure within Figure 6.2.b with a maximum of 3.85V. The same goes for the minimum voltage values. As the second Figure shows a +0.4V shift in heartbeat's voltage there is a different systolic pressure and diastolic pressure. The values would need to be calibrated for each user as the thickness and skin tone of the finger would be relative to the person.

To calibrate for each person would require the mean heart rate value. Figure 6.2.a's value would be at 3.68V and Figure 6.2.b's value would be at 3.72V. The mean value will be relative to the blood pressures' mean value of the midpoint. If the person in Figure 6.2.a's heart beat had a blood pressure at the time of 120/80, we can map out the relative pressures by using the formula [46]:

$$Y = \left(\frac{(x - A)}{(B - A)}\right) \times (D - C) + C \tag{6.3}$$

Where Y is the blood pressure, X is the voltage value, A is the minimum value of the heartbeat, B is the maximum heartbeat value, D is the minimum DBP and C is the maximum SBP. For example, using Figure 6.2.a, we want to find the blood pressure when the voltage is at the mid-point of 3.68:

$$Y = \left(\left(\frac{(3.68 - 3.57)}{(3.8 - 3.57)}\right) \times (120 - 80) + 80\right) \tag{6.4}$$

This gives a pressure of ~100mmHg. We can use the same equation to predict the blood pressure of Figure 6.2.b by replacing X's values with the maximum and minimum voltage to get the pressure to be 128mmHg when the voltage is at 3.85V and 87mmHg when the voltage is at a low of 3.61V leading to an overall pressure of 128/87.

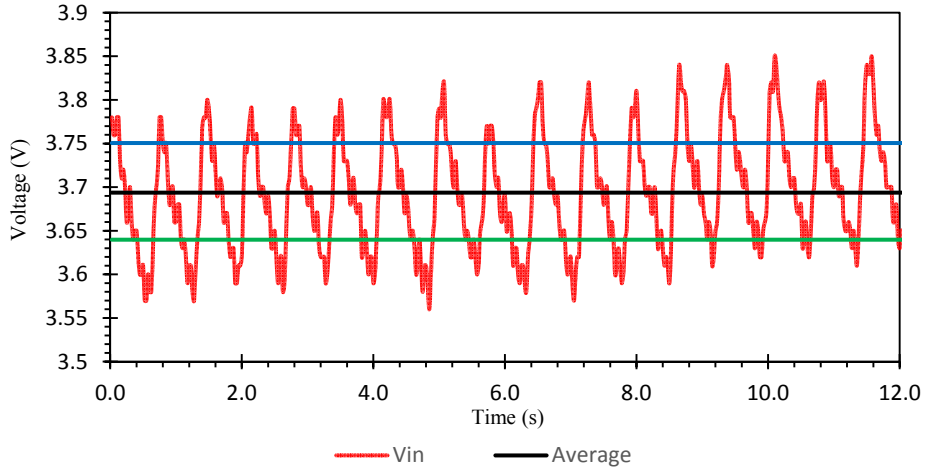

Figure 6.3. graph of the heart rate with average, average high and average low.

Figure 6.3 shows the graph of the continuous heart rate that the proposed heart rate monitor imaged. It shows about 17 heart beats in 12 seconds, leading to a heart rate of 85BPM. As the average heart rate is measured between 60 and 100 beats per minute and the average blood pressure is ~120/80, it is safe to assume that this person's blood pressure could have been 120/80. By taking the average reading of the numbers above the average line (Blue line (AvH)) and taking the average reading of the numbers below the average line (green line (AvL)), we can insert them into the previously stated formula to assume the blood pressure at that moment.

From the above expressions and graph reading, the developed model can be expressed as:

$$BP = \left(\left(\frac{(Vin - AvL)}{AvH - AvL} \right) \times (SBP - DBP) + DBP \right) \qquad (6.5)$$

Where Y has become BP (Blood pressure), X has become Vin (the respective voltage reading from the analogue input), A has become AvL(Average low), B has become AvH (average high), D has become SBP(known systolic blood pressure) and C has become DBP (known diastolic blood pressure).

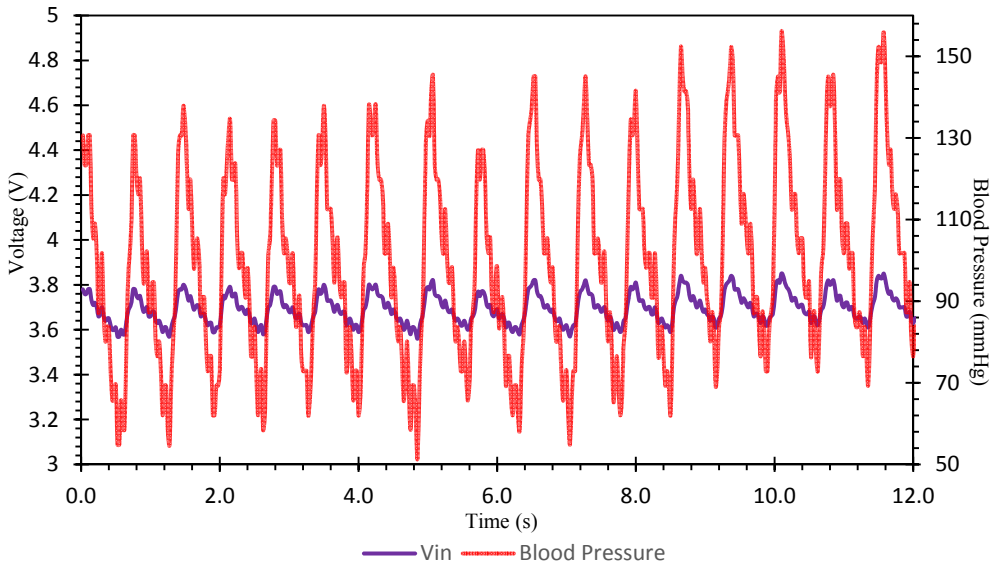

Figure 6.4. A graph of the correlation between heartrate (purple) and blood pressure (red).

The above Figure 6.4 shows the correlation between the heart rate and blood pressure. It shows that the blood pressure is directly proportional to the heart rate.

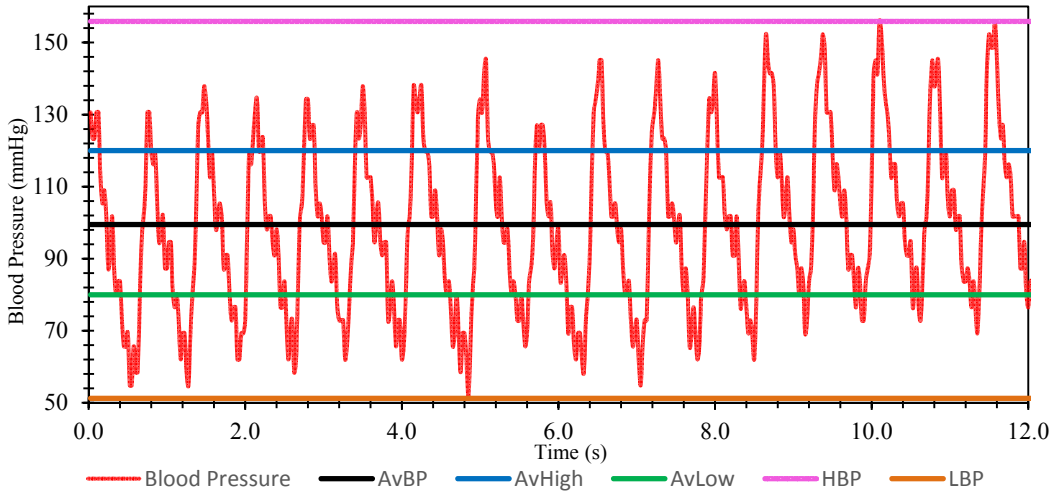

Figure 6.5. A graph of the predicted average blood pressure

Figure 6.5 shows the blood pressure's change against time. It ranges from 50 (orange line) to 150 (pink line).The average blood pressure throughout the 12 seconds was at 99.5mmHg (black line). By taking the average blood pressure above 99.5mmHg, we find the average high to be at 120mmHg (blue line) and by taking the average low of the pressure below the average line, we can obtain an average blood pressure of 80mmHg (green line).

As Diastole occurs for about two thirds of a heartbeat and systolic for the remaining one third , the equation for Mean Arterial Pressure (MAP) is as follows[47].

$$MAP = \left(\frac{\left((2 \times DP) + SP \right)}{3} \right) \tag{6.6}$$

Given that we can assume systolic and diastolic blood pressure from the heart rate, it is also possible to work out the MAP. Figure 6.6's MAP is 93.3mmHg.

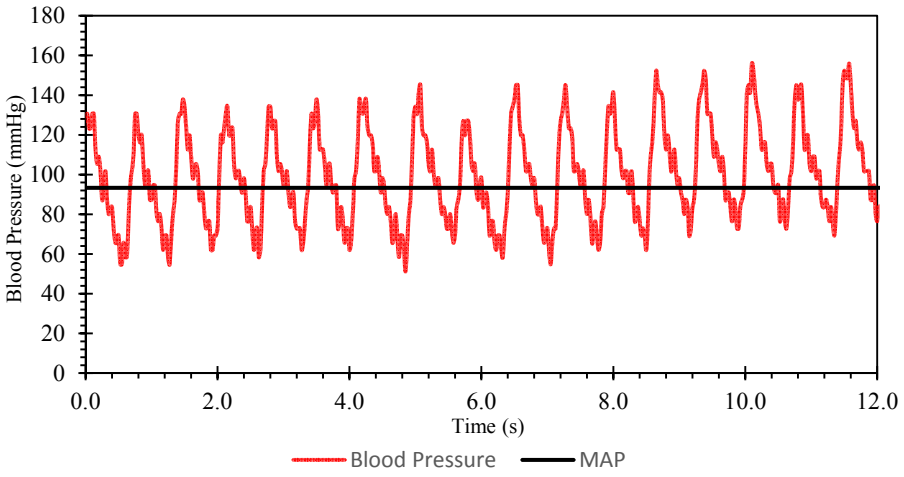

Figure 6.6. A graph of MAP of 93.3% with blood pressure.

To test the possible theory, another heart rate was conducted with the blood pressure known. The blood pressure during the experiment was 133/72. Figure 6.7 shows the heart rate obtained by the heart rate monitor created in Chapter four. The heartrate is at 102BPM.

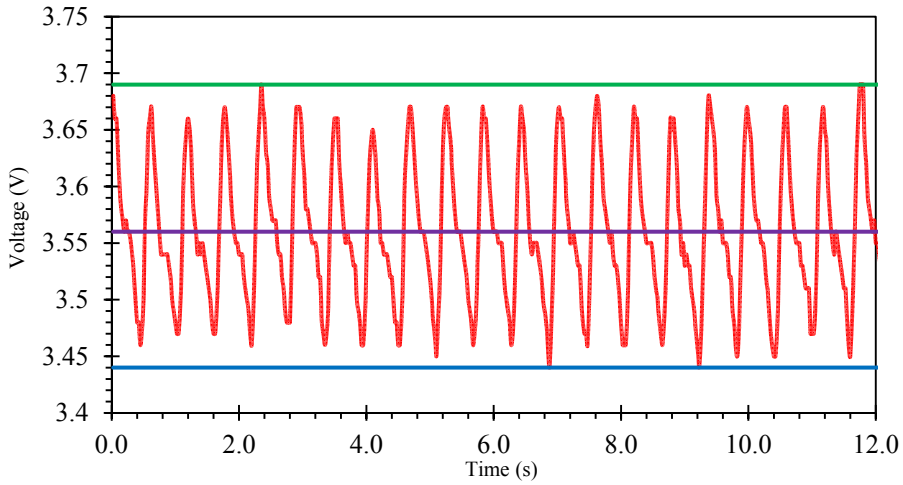

Figure 6.7. another heartrate graph with a heartrate of 102BPM with a blood pressure of 133/72.

The average of the heart rate was taken (purple line) along with the maximum (green line) and minimum (blue line). After finding the average high (3.62V) and average low (3.51V) of the values, it is possible to put the values into the developed formula (6.5).

Where AvL is 3.51, AvH is 3.62, SBP is 133 and DBP is 72. The measurement predicted that the average high (systolic blood pressure) was 133mmHg and the average low (diastolic blood pressure) was at 72mmHg.

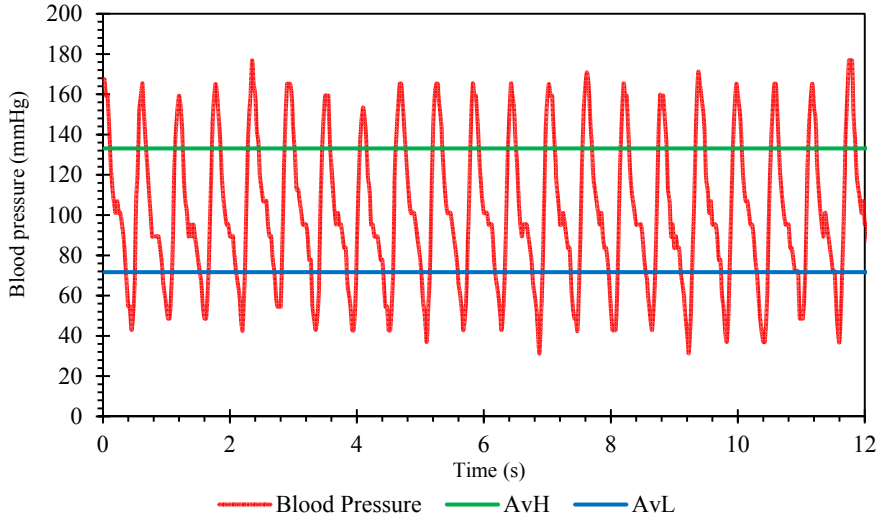

Figure 6.8. The blood pressure's calibration graph.

Now the calibration for the blood pressure has been applied, we can predict the blood pressure with a different heart rate as shown in Figure 6.9.

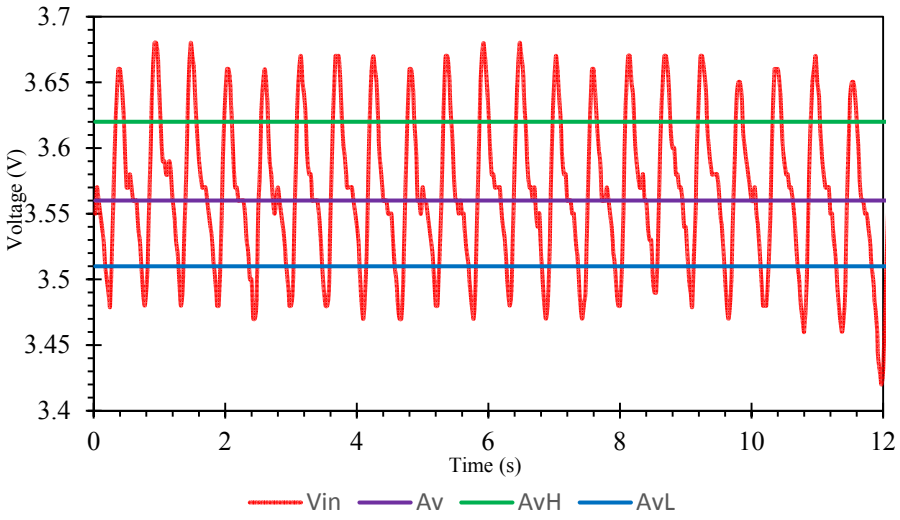

Figure 6.9. Graph of a heart rate of 105BPM.

The values were added to the calibrated formula (6.6) which predicted a blood pressure of 133.5/77. The real value of the blood pressure was 137/77. Showing a 97.4% accuracy compared to the benchmark blood pressure monitor. The result gave a MAP of 95.9mmHg. Only 1.45% away from the real 97.3mmHg MAP.

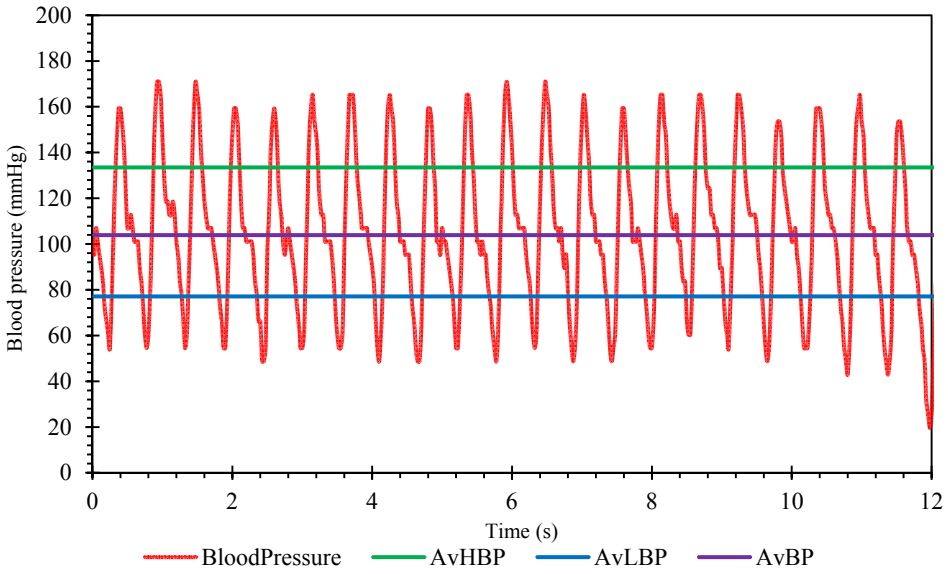

Figure 6.10. The heartrate's values placed in the formula to give the predicted blood pressure of 137/77.

Another experiment of heart rate 95BPM predicts a blood pressure of 147.5/77 shown in Figure 6.11. The real blood pressure value wat as 160/86, giving a benchmark MAP of 110.7mmHg and a predicted MAP of 100.5mmHg. Although there is a larger error of 9.2% within MAP, 7.8% error within systolic prediction and a 10.5% error with diastolic pressure prediction, this graph can still represent that there is an apparent correlation between the blood pressure and the heart rate resistance values. The heart rate has not needed to increase dramatically to also produce a high blood pressure. The heart rate is at an average level but the systolic blood pressure is higher than it should be. Other unknown variables must take into consideration the overall systolic and diastolic pressures though this method has demonstrated that the blood pressure has definitive correlation with the amplitude of the voltage received. The blood pressure value does not affect the heart rate and can be calculated independent of heart rate.

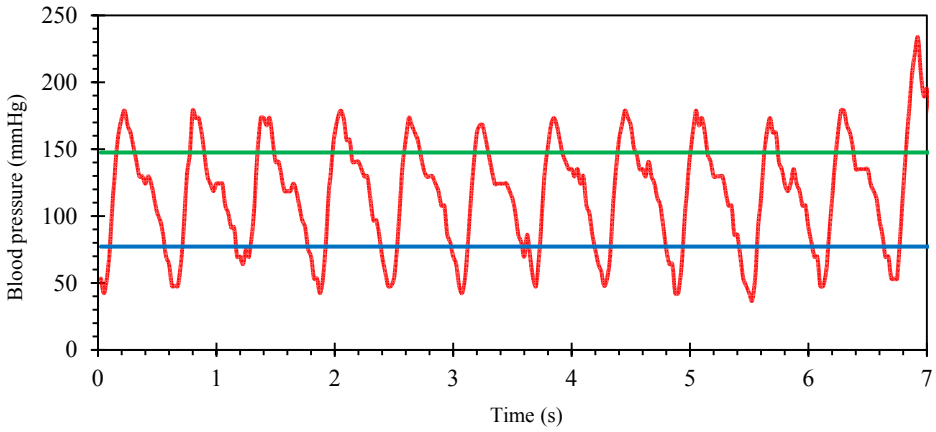

Figure 6.11. A graph showing heart rate at 95BPM with blood pressure 147.5/77.

Pearson's product moment correlation coefficient can be used to obtain the linearity of the average voltage and the blood pressure [41]. By taking the average voltage of the heart rate monitor after five hundred samples and recording the blood pressure on a bench mark device, we can compare the correlation. The resulting value *r* will produce a value between -1 and 1. If the *r* is equal to 1, the two variables show strong linear correlation and if the value is close to -1, the values can be considered highly negatively correlation. A value of 0 shows no correlation. Considering that the systolic and diastolic values are difficult to compare with one variable (the average value), we can compare the average voltage with the MAP (as can be seen in equation (7)).
By taking the Y values (Average voltage of 500 samples (12.5 seconds recording the values)) and the X values (MAP), we can insert them into the formula: $r = s_{xy} / \sqrt{s_{xx} s_{yy}}$ by using the following equations:

$$S_{xy} = \sum xy - \frac{\sum x \sum y}{n}; \qquad S_{xx} = \sum x^2 - \frac{\left(\sum x^2\right)}{n}; \qquad S_{yy} = \sum y - \frac{\left(\sum y^2\right)}{n}; \tag{8}$$

where Σx is the sum of all of the MAPs, Σy is the sum of all of the average voltage values, Σx^2 is the sum of all of the MAP values squared, Σy^2 is the sum of all of the average voltage values squared, Σxy is the sum of all of the MAP values multiplied by the average voltage values and *n* is the total number of variables. Table 6.1 below shows the values of *X, Y, X2, Y2,* and *XY* values used for the formulas and Table 6.2 shows the sum products; Σx, Σy, Σx^2, Σy^2, Σxy and *n*.

Table 6.1. X and Y values used to calculate the product moment correlation coefficient

MAP	AvVal	X^2	Y^2	XY
110.333333	3.55511022	12173.444	12.6388087	392.24716
110.666667	3.570320641	12247.111	12.7471895	395.11548
111	3.565751503	12321	12.7145838	395.79842
79	3.448416834	6241	11.8915787	272.42493
81.3333333	3.438557114	6615.1111	11.823675	279.66931
82.3333333	3.444749499	6778.7778	11.8662991	283.61771
88	3.448857715	7744	11.8946195	303.49948
91.6666667	3.440420842	8402.7778	11.8364956	315.37191
102.333333	3.509579158	10472.111	12.3171459	359.14693
102	3.467755511	10404	12.0253283	353.71106
92	3.501202405	8464	12.2584183	322.11062
92.3333333	3.444629259	8525.4444	11.8654707	318.0541
93	3.434448898	8649	11.7954392	319.40375
97	3.518456914	9409	12.3795391	341.29032

Table 6.2. The sum products and *n* used for the formulas.

ΣX	ΣY	ΣX^2	ΣY^2	ΣXY	N
1333	48.7883	128447	170.055	4651.46	14

The results proved S_{xy} to be 6.12, S_{xx} to be 1526 and S_{yy} to be 0.0336. The calculated *r* value is 0.86. This shows that there is strong correlation between the change in average voltage and the change in the MAP.

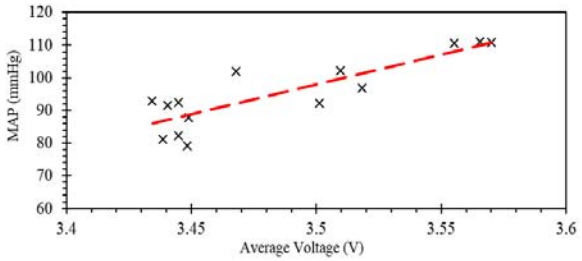

Figure 6.12. A graph of average voltage and MAP.

Figure 18 shows the mean arterial pressures ranging from 79 to 111mmHg against the average voltages ranging from 3.43V to 3.57V. Considering the Arduino microcontroller can only take values to two decimal places, correlation can be seen with the values. If the voltage could be measured over a smaller scale, the values would be more spread apart.

Using Figure 6.12, and equation (6), Y = MX + C formula can be used to predict a mean arterial pressure with voltages, where Y is the average voltage, X is the MAP, M is the gradient (187.09) and C is the Y intercept (-556.41). The formula is now Y = 187.09X – 556.41. Figure 6.13 illustrates the real values calculated (red line) and the predicted values from the equation. An average voltage of 3.40 will predict a MAP of 79.70mmHg, an average voltage of 3.50V will predict a MAP of

98.41mmHg and a voltage of 3.60 will predict a MAP of 117.1. This shows that for every 0.1V change in average voltage, 18.7mmHg change in MAP can be seen. This could be reason why Figure 6.12's clustering results differ from 79mmHg to 90mmHg with only a 0.02V range. Sample four showed an error of 12% which is quite large however the rest of the results were never more than 7% off. As a preliminary experiment, the obtained results clearly demonstrated correlation between the voltages received from the heart rate monitor and the real benchmark blood pressure.

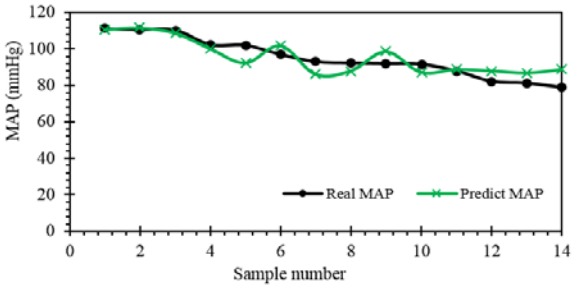

Figure 6.13. Real mean arterial pressure values (black line) against the predicted values (green line).

Since we can predict the MAP, we can try to predict the systolic pressure (SP) and diastolic pressure (DP) using the MAP's results. By dividing each value's real systolic pressure by the real MAP, we get a value between 1.40 and 1.46. This value can be averaged out to become 1.4307 (SPk). The same can be carried out by dividing the real diastolic value by the MAP to gain an average of 0.7846 (DPk). When the averaged SPk value is multiplied by the predicted MAP, we gain a predicted SP value and when the DPk value is multiplied by the MAP, we gain a predicted DP value. Table 6.3 shows the Real MAP values, predicted MAP values and the accuracy off the predicted values with the real MAP values.

Table 6.3. A table of the Real MAP (mmHg) values with the Predicted Values (mmHg) and the Accuracy of the values (%).

n	Real MAP	Predict Map	MAP%
1	110.33	108.72	1.47
2	110.67	111.56	0.81
3	111	110.71	0.26
4	79	88.75	12.35
5	81.33	86.91	6.86
6	82.33	88.07	6.97
7	88	88.84	0.95
8	91.67	87.26	4.81
9	102.33	100.20	2.09
10	102	92.37	9.44
11	92	98.63	7.21
12	92.33	88.05	4.64
13	93	86.14	7.38
14	97	101.86	5.01
			5.02%

Figure 6.14. a) illustrates the real SP values with the predicted values, it is clear from this figure that the values are very close to the real SP values. The red markers show that as the real SP values decrease, so do the predicted values. The accuracy testing of the predicted values to the real values revealed an overall accuracy of ±5% with the least accurate value being 12% off its true value (14th sample) and the most accurate being 0.24% off the real value. The diastolic values could also be predicted to ±5.1% accuracy of real value, as shown in Figure 6.14. b) with very similar correlation.

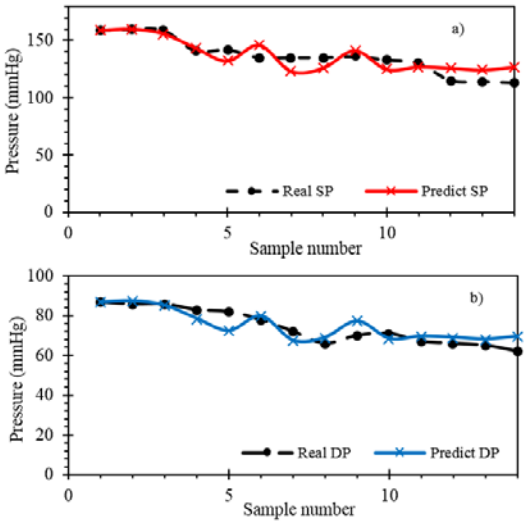

Figure 6.14. a) Real systolic pressures (black short dashed line) with the predicted SP pressures (red markers). b) Real diastolic pressures (black long dashed line) with the predicted DP pressures (blue markers).

Figure 6.15 shows the overall accuracy of the MAP, SP and DP real, and predicted values. The black dotted line shows the real SP values, the black line is the real MAP values, the black dashed line is the real DP values, the red markers are the predicted SP values, green markers are the predicted MAP values and the blue markers are the predicted DP values.

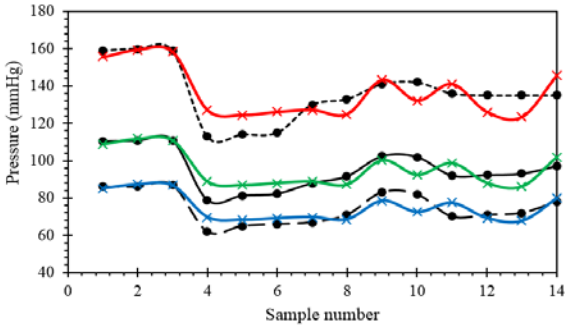

Figure 6.16. A graph of all of the real pressures (Systolic (black short dashed line), mean arterial pressure (black line) and diastolic pressures (black long dashed line)) with the predicted values (systolic (red), MAP (green) and diastolic (blue).

Figure 6.17 a) shows an image of the experiment set up with the blood pressure blocking the left brachial artery. The heart rate device is on the index finger of the

right hand sending the changes in voltages to the Arduino's serial monitor for later analysis. Figure 22 b illustrates the proposed schematic diagram of the system predicting the MAP, SP and DP.

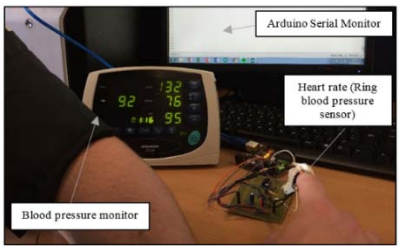

Figure 6.17 a). Experiment set up of the measurement blood and the ring sensor measuring the blood pressure.

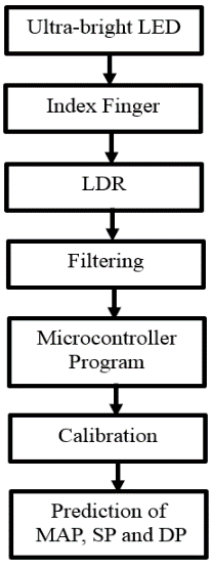

Figure 6.17.b Schematic diagram of the system from the LED input to the prediction of the MAP, SP and DP.

It is clear to see that there is a correlation between the average heart rate and the corresponding real time blood pressure. Our experiment demonstrates that as there is more blood flowing through the finger, there is a higher voltage received at the heart rate monitor. The higher the voltage received, the higher the corresponding blood pressure of the user. Figure 23 shows a graph of four participants' average voltages taken throughout the day against the real MAP. It is clear to see that there is correlation strong between the voltage and the blood pressure. Each participant (PPT) was of different race to show that the amplitude of the average voltage will change each person's calibration with tone of the skin and thickness of the finger. The voltages show that as the voltages increase, the MAP also increases. A Pearson's product moment correlation coefficient was taken for each participant. The first participant (red line (MAP) and red dashed line (Vin)) has a correlation of 0.88. The second participant (green line (MAP) and green dashed line (Vin)) has a correlation of 0.924. The third participant (blue line (MAP) and blue dashed line (Vin)) has a correlation of 0.78 and the fourth participant (purple line (MAP) and purple dashed line (Vin)) has a correlation of 0.90. The overall average correlation of the participants is 0.87 which suggests strong positive correlation. The values

can be found below in table 6.4.

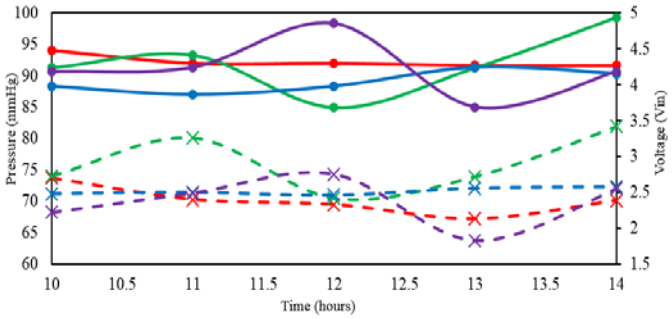

Figure 6.18. A graph of four participants' real MAP against the average voltage.

Table 6.4. A table showing four participants' real mean arterial pressure (MAP) values with the average voltage (Vin) for four participants measured from 10:00am to 14:00pm.

Time	MAP1	Vin1	MAP2	Vin2	MAP3	Vin3	MAP4	Vin4
10:00	94	2.7	91.333	2.73	88.333	2.48	90.6667	2.22
11:00	92	2.4	93.333	3.26	87	2.5	91.333	2.49
12:00	92	2.33	85	2.42	88.333	2.46	98.333	2.75
13:00	91.6667	2.13	91.3333	2.72	91.333	2.56	85	1.83
14:00	91.6667	2.39	99.333	3.42	90.33	2.58	90.6667	2.55

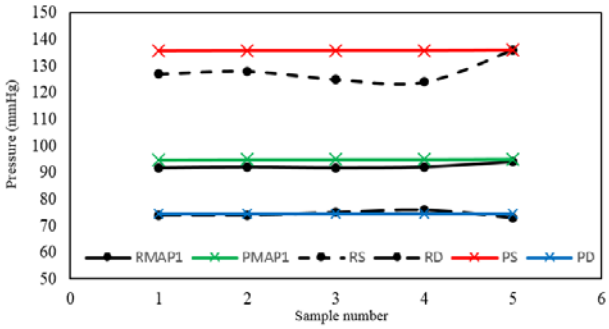

Figure 6.19. A graph of the real MAP of the first participant's real pressures (real systolic (RS, black small dashed line), real MAP (RMAP1, black line) and diastolic (RD, black large dashed line)) with the predicted pressures (predicted systolic (PS, red line), predicted MAP (PMAP1, green line) and predicted diastolic (PD, blue line)).

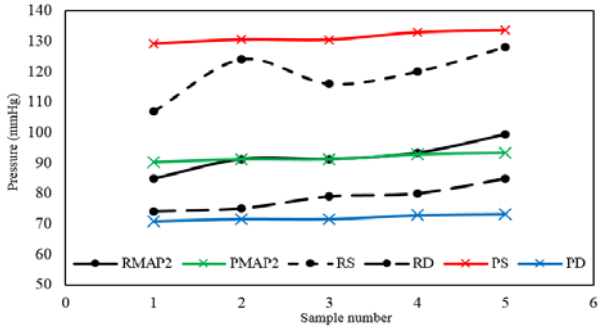

Figure 6.20. A graph of the real MAP of the second participant's real pressures (real systolic (RS, black small dashed line), real MAP (RMAP2, black line) and diastolic (RD, black large dashed line)) with the predicted pressures (predicted systolic (PS, red line), predicted MAP (PMAP2, green line) and predicted diastolic (PD, blue line)).

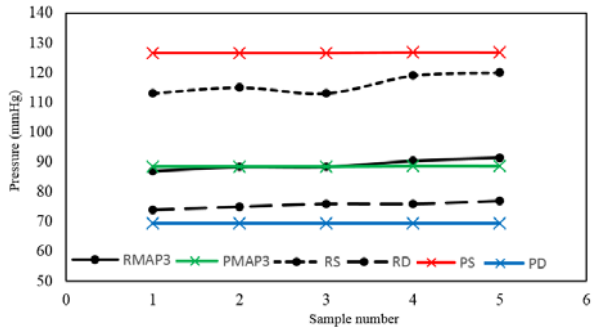

Figure 6.21. A graph of the real MAP of the third participant's real pressures (real systolic (RS, black small dashed line), real MAP (RMAP3, black line) and diastolic (RD, black large dashed line)) with the predicted pressures (predicted systolic (PS, red line), predicted MAP (PMAP3, green line) and predicted diastolic (PD, blue line)).

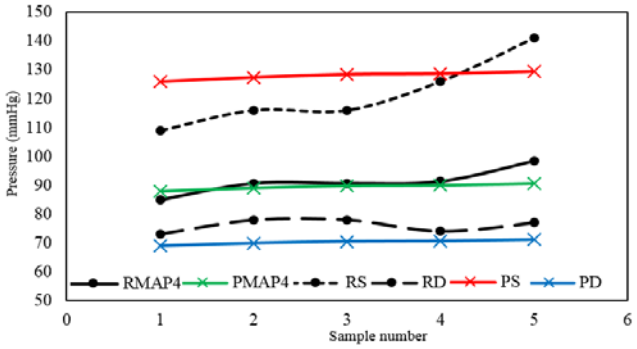

Figure 6.22. A graph of the real MAP of the fourth participant's real pressures (real systolic (RS, black small dashed line), real MAP (RMAP4, black line) and diastolic (RD, black large dashed line)) with the predicted pressures (predicted systolic (PS, red line), predicted MAP (PMAP4, green line) and predicted diastolic (PD, blue line)).

Figures 6.19-6.22 show the four participant's real pressures against the predicted pressures. The first and third participants claimed to have not eaten anything during the course of the day. This would explain why the values remain at a steak level. All of the systolic and diastolic pressures seem to be slightly off though do resemble over 90% accuracy of the predicted pressures. The same SPk and DPk values were used to calibrate the systolic and diastolic pressures and may need more results to gain a more accurate value. All of the predicted mean arterial pressures were over 93% accurate which suggests that there is correlation between the average voltage of the heart rate monitor and the mean arterial pressure. In regards to the mean arterial pressure, PPT 1 has a real MAP range of 91.667-94mmHg and a predicted range from 94.8-95.12, an overall average accuracy of 97% throughout the five hours. PPT 2 has a real MAP range of 85-99.33mmHg and a predicted range from 90.29-93.36mmHg, an overall average accuracy of 99% throughout the five hours. PPT 3 has a real MAP range of 87-91.33mmHg and a predicted range from 88.53-

88.60mmHg, an overall average accuracy of 99% throughout the five hours. PPT 4 has a real MAP range of 85-98.33mmHg and a predicted range from 88.0-90.51mmHg, an overall average accuracy of 98% throughout the five hours. It is clear to see that the five tests did not produce results with more diverse values. If the ranges of the participants were longer, the calibration of the participants would have produced more accurate results like Figure 6.16. Figures 6.19-6.22 use the same calibration techniques as Figure 6.16 and uses the changes in the average voltage to view the change in blood pressure.
Figure 6.24 illustrates the measurements of one participant blood pressure which is carried out from 10:30h till 14:30h. It shows the blood pressure changing against the predicted values. After further calibration, the average MAP of the four hours was at 98.92mmHg and the average predicted MAP over the four hours was at 92.8mmHg (93.8% accurate). The average real systolic pressure was at 144.25mmHg and the predicted average systolic pressure was at 132.77mmHg (92% accurate). The average real diastolic pressure was at 76.25mmHg and the predicted diastolic pressure was 72.7mmHg (95.5% accurate). The participant had lunch at 13:00h and it is clear to see from the graph an increase in real and predicted blood pressure (at 13:30) and restores back to near the average values at 14:00h. Our developed experiment proves that continuous monitoring of the blood pressure with this device throughout the day and night is definitely possible after miniaturisation.

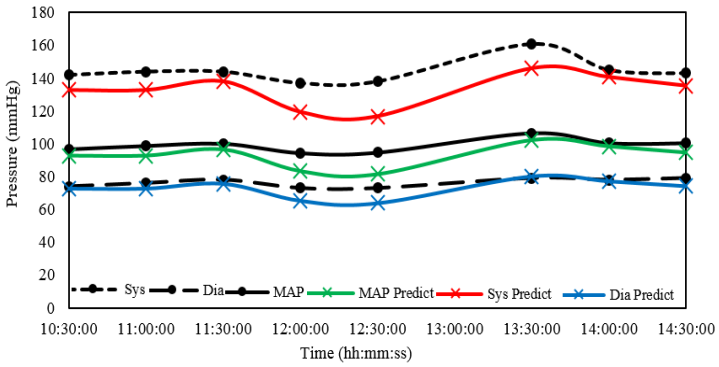

Figure 6.24. Graph of real MAP (black line), systolic (black short dash) and diastolic (black long dash) pressures with the predicted; MAP (green line), systolic (red line) and diastolic (blue line) against time from 10:30am to 14:30pm.

The average real heart rate throughout the experiment ranged from 74-108BPM and the predicted heart rate ranged from 77.7-115.2BPM. The heart rate accuracy throughout the experiment was at 104%. This shows that slight calibration within the programming is required though it is still highly accurate.

6.4 Blood Pressure Summary

In this research paper we have proposed and demonstrated a novel continuous monitoring of the blood pressure using simple and low cost heart rate ring sensor device. We have demonstrated that it could be possible to obtain a predicted blood pressure using the proposed heart rate device. We show that when more blood is

flowing through the finger (more blood in the finger), less light is received by the LDR which created a larger resistance. As there is a larger resistance, there is a higher blood pressure. The mean arterial blood pressure can be predicted with aid of the photoplethysmography, and systolic and diastolic pressures can be predicted with use of the MAP to 5% of their real values. This method uses a different technique of measuring blood pressure compared with the current devices that still use the cuff method like the Nonin 2120 benchmark blood pressure device [30]. Not using the cuff method and having a continuous blood pressure measurement throughout the day will eliminate any issues patients may have when having their blood pressure taken. This method will enable continuous monitoring of the blood pressure where the medical examiners will be able to view how a patient's blood pressure changes throughout the day and gain a true value of the average blood pressure as food, caffeine and other variables have high effects on the blood pressure. This novel device is extremely affordable using basic filtering and amplification techniques. In this paper we show that there is strong linear correlation between the amplitude of the voltage received and the blood pressure, enabling to build the continuous blood pressure sensor. The proposed blood pressure device is tested and benchmarked, against Nonin 2120 [30], for four participants for a continuous period of four hours, where the demonstrated accuracy between real average MAP (using Nonin 2120), and the average predicted MAP, using our proposed device, is 93.8%. The demonstrated device accuracy between average real systolic pressure (using Nonin 2120) and the predicted average systolic pressure was 92%. The demonstrated device accuracy for the average real diastolic pressure (using Nonin 2120) and the predicted diastolic pressure is 95.5% for four participants in the period of four hours.

Chapter 7

7.0 Electrocardiography

This chapter will discuss another sensor that could be implemented to use with the proposed ring device. This is an Electrocardiography monitor with use of two ringed devices.

7.1 Electrocardiography Introduction

Electrocardiography (EKG or ECG) is an electrical activity test of the heart. It is used to find problems with a patient's heart and aid diagnosis following reported symptoms (inter alia) pain, arrhythmia, breathlessness within the patient potentially caused by heart attack, heart disease, inflammation of the sac surrounding the heart (pericarditis), or angina [48].

Either, ten, five or three nodes are placed on a patient to view the different planes of the heart for a non-invasive measurement [49]. The readings of the polarisation are then recorded. An ECG wave can be split into different stages; P, Q, R, S and T. Action potentials of the heart's sinoatrial (SA) node spread towards the atrioventricular (AV) node leading to atrial depolarisation. This atrial depolarization induces atrial systole and is seen as the P wave. The action potentials then spread through the bundles of the heart causing ventricular depolarisation and induces ventricular systole. This is seen as the QRS complex on Figure 7.1 [50]. As the action potentials pass out of the ventricles, ventricular diastole is then induced and ventricular repolarization is shown by the T wave [51].

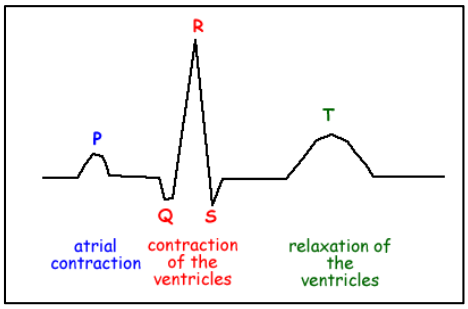

Figure 7.1. The resultant line of an ECG measurement of one heartbeat.

An ECG is a more accurate value of heart rate. There is an iPhone case that is able to tell the user's ECG by placing their thumbs on each side of the case [52]. This uses the 'three lead' method and measures the potential difference of the electrical pulses within the thumb. The information is read by the phone to the app and can be recorded by the user. This does assume that the user will have to own an iPhone in the first place (which are £500 plus). Having ECG within the proposed ring will

free the user from having to purchase a specific phone case and iPhone. It will also be able to inform the user when it is time to take the ECG reading.

The multisensory device will be able to use many of the same embedded technologies to produce all of these vitals readings to then be sent to a server, nominated individual or healthcare professional or logged. The target market is the elderly and so many could be frustrated by using the current iPhone technologies and systems and the proposed device takes the responsibility for taking the measurements away from the individual and into the hands of their carers or health professionals.

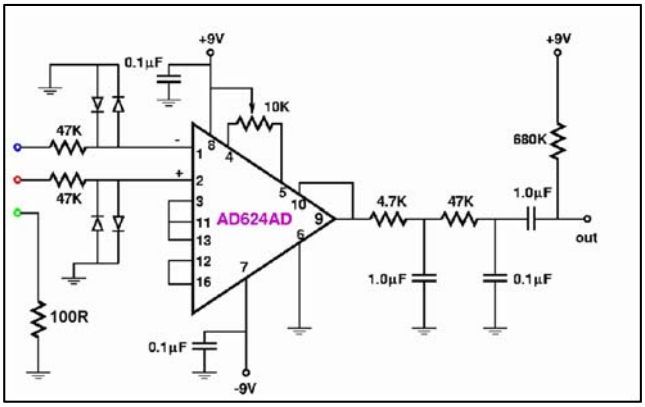

Figure 7.2. ECG electronic circuit diagram.

Figure 7.2 shows a circuit diagram of a three lead ECG monitor [53]. One of the nodes is attached to a finger on the left hand and the other will be attached to a finger on the right. The third lead is grounded to form a base line of the user. This technique will allow the circuit to be integrated into the ring device. The user will require two rings for the measurement where the ground pin is integrated into at least one of the rings.

Utilising technology similar to that which the iPhone case uses, the ring would be paired with another ring, worn on the other hand, so as to find the ECG. A cable between the two may be needed to connect the nodes and calculate the potential difference of the two fingers. This can be easily achieved as the ECG is generally only measured on demand rather than on a continual basis.

The ECG could be measured after a user has taken medication. This will enable the user to view the effects of the medication on their heart.

Chapter 8

8.0 Conclusion

Within this thesis, several health sensor technologies have been reported and implemented:

The heart rate monitor has been implemented as a ring device using PPG's transmissive mode method. The signal was filtered and amplified and produced accurate results. The heart rate monitor is extremely affordable and can be miniaturised even further to fit into a ring.

The LM35 temperature sensor has been programmed and calibrated to the user and showed successful results in determining the body temperature. No new technologies have come from this and many body thermometers use LM35 transistors to find the body temperature. Further design would have to be considered to fit the device securely into a ring.

An alternative method of measuring SpO2 has been discussed and implemented. Instead of using the absorption differences of oxyhaemoglobin and deoxyhaemoglobin, the proposed sensor measures how red the blood is. The more oxygen within the blood, the brighter the blood colour will appear. Because the colour is brighter this signifies that the 'red value' has decreased towards the orange spectrum and the SPo2 level will be higher. If the blood has less oxygen, it is a darker red; and the red value will increase (towards the IR spectrum) showing a reduction in the SpO2. Therefore, we can measure a change in oxygen levels by measuring the colour of the blood.

The results of the heart rate monitor showed that it could be possible to see correlation between the heart rate's voltage amplitude and blood pressure. If blood pressure was above normal, there will be more blood between the LED and LDR. As there is more blood, less light will get through to the LDR. As there is less light,

there is a higher resistance. This change in resistance can be measured and calibrated, with further work, to produce a more accurate blood pressure estimation although this research shows the initial and potential for correlation.

There is potential to introduce an electrocardiography device into the overall ring device though would require two rings to be work when measured.

There is still much work to be done including integrating all of the sensors together and obtaining continuous results.

The novelty of this work would be the production of all of the sensors integrated into one device. By using the PPG methodologies, the heart rate, SpO2 and potentially the blood pressure and ECG could use similar, affordable components and therefore miniaturizing the ring device. Alongside with the body temperature and electronic pillbox, the overall device would enable and aid for continuous health monitoring and patient status within the home.

Chapter 9

9.0 Future Work

This thesis has demonstrated ways of producing sensors that measure body vitals. The main aim of the future work chapter will be how to combine the sensors into one ring device that will be able to measure heartrate, oxygen saturation, body temperature and potential for blood pressure. Combining all of the sensors and enabling users to wear the device throughout the day will produce a general view of their physical condition. By continuously monitoring heartrate it is possible see how active the user is and how well their sleep cycle is.

Patients with sleep apnoea will be able to wear the ring device during sleep comfortably with continuous health monitoring. If the device notes a higher heart rate and a lower oxygen level, it will be able to enable appropriate measures or action.

An electronic pill box has been created which is programmed to the user's medication routine. When it is time for the user to take medication, it will send a

radio frequency (RF) signal to a bracelet, worn by the user with range of over 30 metres. They can approach the pill box, view which medication and how many to take on a screen readout and press a button to turn off the red LED on the bracelet device. As medication can be extremely sensitive, it is important that the user doesn't forget to take the medication, it is also equally important that the user takes the right amount of medication as some can be highly toxic in excess. The pillbox device will update how many pills they have left and can inform the user when to pick up some more. The pillbox can also send a text/email to a relative or an appropriate medical helper to inform that the user has not taken the medication and can send a request for repeat prescriptions when supplies are low.

The future work will combine the pillbox with the proposed ring device. This will allow the pillbox to also know the heartrate, body temperature, blood pressure and SpO2 of the user so that it can become aware if any of the medication has any damaging effects. Warfarin, for example, thins the blood and can be toxic if taken in excess. The pill box will know when the user has taken their medication and can view how the medication affects the vitals of the user. This can enable a doctor or other medical practitioner to prescribe different levels of the said drug or inform them to take it at a different time of day. The medic will be able to add, edit or remove prescribed drugs. The medical professional will be able to update the user's pillbox with the new drug time so the user will not panic or worry when it is time to take the medicine. If a patient has become unwell, the doctor will be able to view which drugs have been taken and view a profile of the patient's prior medical and vitals history.

For all of this to happen, a database will need to be created which can record each user's vitals securely. The ring device will also need to be able to connect to the internet. As the device is aimed at users within the home, a base station device (such as the pillbox device) can be implemented which can receive, store and send the information. The ring device will need to be able to store the data until it is within range of the base station. A RTS/CTS (request to send/ clear to send) protocol can be implemented and the ring device can have a transceiver recognise when the base station device is nearby and if it is able to send the information.

The ring device will need to be worn all day long and must therefore have an appropriate battery life. Not sending the information to the database itself will save much energy and ensure that it can use the battery for measuring the vitals and sending the data securely to a receiving base station. As a person's hand moves quite a lot during the day, energy harvesting of kinetic movement could be implemented in a similar way to that used by watches. As mentioned within the ECG section, a user could have another monitoring ring. The user could use one ring whilst another is charging and use both when measuring ECG.

Chapter 10

10.0 Appendices

This chapter shows the programming code for the Heart rate and Temperature sensor.

10.1 Appendix 1

```
//Code for heart rate monitor.

#include "Timer.h"                    //Timer library for stopwatch

#include <LiquidCrystal.h>                    //LCD library


LiquidCrystal lcd(12, 11, 5, 4, 3, 2);          //LCD pin array set up

Timer t;                          //Name the timer; t

float timer = 0;                          //Give avariable for the timer

const int numReadings = 40;       //Number of readings in moving average

float readings[numReadings];      //The readings from the analog input

int readIndex = 0;                 //The index of the current reading

float total = 0;                          //The running total

float average = 0;                        //The average

float averageVoltage = 0;         //The voltage - the average number will reduce a
                                    //number +-0

int counter = 0;                   //To count the beats

int counterTwo = 0;               //Monitor weather the averageVoltage is >||< than
0

float heartRate = 0;               //To use for the heart rate value
```

```
float Vth = 0.1;                        //Voltage threshold


void setup()
{
  Serial.begin(9600);                                  //Begin the serial monitor
  lcd.begin(16, 2);                                    //Begin the LCD screen
  t.every(1000, takeReading);                          //Setup a timer that increments
every 1000 ms (1s)
  for (int thisReading = 0; thisReading < numReadings; thisReading++)
 //Reset the reading number once reached a maximum
  {
    readings[thisReading] = 0;
  }
}
void loop()
{
 int sensorValue = analogRead(A0);                 //Read the A0 pin conected to the
                                                     //output of the HR monitor
  float voltage = sensorValue * (5.0 / 1023.0);    //Convert the analog reading (which
goes from 0 - 1023) to a voltage (0 - 5V):
   total = total - readings[readIndex];           //Subtract the last reading
  readings[readIndex] = voltage;                  //Read from the sensor
  total = total + readings[readIndex];           //Add the reading to the total
```

```
 readIndex = readIndex + 1;                    //Advance to the next position in the
array


 if (readIndex >= numReadings)                 //if we're at the end of the array;
{
   readIndex = 0;                                    //Wrap around to the
beginning
}


average = total / numReadings;                       //Mean average is the total /
number //of readings
averageVoltage = ((voltage - average) );                 //Produces value near 0


if (counterTwo == 0 && (averageVoltage >= Vth))     //If the average voltage is >=
the Vth
{
 counter++;                              //Record one beat
 counterTwo = 1;       //Increment the second counter to ensure only one //value
above Vth is noted
}
else if (counterTwo == 1 && (averageVoltage <= -Vth))     //If the average voltage
// is >= the Vth
{
counterTwo = 0;                                  //Reset the counter ready for another
```

```
beat
}
t.update();                                    //Update the timer
heartRate = counter / (timer/60);       //Heartrate = noted beats per minute


if (counter == 30)                             //If the has noted 30 beats
{
  counter = 0;                                 //Reset counter
  timer = 0;                                   //Reset timer
  lcd.clear();                                 //Clear the LCD screen
   lcd.setCursor(0, 0);                        //Set LCD cursor to the first space on the
first line
   lcd.print("Heart Rate: ");                 //Print out "Hearrt rate: "
   lcd.setCursor(0, 1);                        //Set cursor to the first space on the second
line
   lcd.print(heartRate);                       //Print the heart rate
   lcd.print(" BPM");                          //Print the units
}
 Serial.print(voltage);                        //Print the voltage
Serial.print("  ");
Serial.print(average);                         //Print the average
Serial.print("  Heart Rate:   ");
Serial.print(heartRate);                       //Print the Heart rate
```

```
Serial.print(" BPM   ");                    //And its units
Serial.print("  ");
Serial.print(counter);                      //Print the counter value
Serial.print("  ");
Serial.print(timer);                        //Print the stopwatch
Serial.print("   ");
Serial.println(averageVoltage);             //Print the averageVoltage
delay(100);                                 //Wait 0.1 seconds
}
void takeReading()
{
timer++;                                    //Increment timer
}
```

10.2 Appendix 2

```
//Code for temperature sensor.

int val;                        //Declare the value

int tempPin = A1;               //Declare the pin number for sensor


const int numReadings = 20;     //Number of readings in moving average

float readings[numReadings];    //The readings from the analog input

int readIndex = 0;              //The index of the current reading

float total = 0;                //The running total

float averageTemp = 0;

const float M = 0.2055;          //Calibrated gradient value

const float C = 30.105 ;        //Calibrated Y intercept value.


void setup()

{

 Serial.begin(9600);

  for (int thisReading = 0; thisReading < numReadings; thisReading++)

//Reset the reading number once reached a maximum

  {

    readings[thisReading] = 0;

  }

}
```

```
void loop()
{
val = analogRead(tempPin);                  //Read the sensor pin
float mv = ( val/1024.0)*5000;              //Convert from analogue to volts
float cel = mv/10;                          //Turn into Celcius
 total = total - readings[readIndex];       //Subtract the last reading
 readings[readIndex] = cel;                 //Read from the sensor
 total = total + readings[readIndex];       //Add the reading to the total
 readIndex = readIndex + 1;                 //Move to the next position in array

 if (readIndex >= numReadings)              //If we're at the end of the array…
{
   readIndex = 0;                           //Wrap around to the beginning
}
averageTemp = total / numReadings;          //Run the average temperature

float tempmx = (M * averageTemp);           //Multiply value by the gradient
float tempmxc = tempmx + C;                 //Add the Y intercept value
Serial.print(tempmxc);                      //Print the new calibrated temperature
Serial.println();                                   //Print a new line
delay(500);                                         //Wait 500ms
}
```

Chapter 11

11.0 Bibliography

[1] F. Huang, P. Yuan, K. Lin, H. Chang, and C. Tsai, "Analysis of Reflectance Photoplethysmograph Sensors" International Journal of Medical, Health, Biomedical, Bioengineering and Pharmaceutical Engineering **5** 622-625, (2011).

[2] J.K.N Mazima, M.Kisangiri and D.Machuve, "Deign of Low Cost Blood Pressure and Body Temperature interface" International Journal of Emerging Science and Engineering **1,** 109- 114, (2013).

[3] R.Klingenberg, "Ring Size Chart" [Online] Available at: http://jewelrymakingjournal.com/ring-size-chart/ (2015).

[4] S. Profis, "Do Wristband Heart Trackers Actually Work? A Check-up", [Online] Available at: http://www.cnet.com/news/how-accurate-are-wristband-heart-rate-monitors/ (2014).

[5] E. Laskowski, "What's a normal resting heart rate?" [Online] Available at: http://www.mayoclinic.org/healthy-lifestyle/fitness/expert-answers/heart-rate/faq-20057979 (2015).

[6] "Your heart rate. What it means, and where on Apple Watch you'll find it.**",** [Online] Available at: https://support.apple.com/en-gb/HT204666 (2015).

[7] "Withings Aura Smart Sleep System", [Online] Available at: http://www.apple.com/uk/shop/product/HFDQ2ZM/B/withings-aura-smart-sleep-system?fnode=82 (2015).

[8] "Fitbit Store" [Online] Available at: https://www.fitbit.com/uk/store# (2015).

[9] "The ultimate fitness super watch" [Online] Available at: http://www.fitbit.com/uk/surge (2015).

[10] S. Richard, “The real world wrist-based heart rate monitor test: Are they accurate enough?” [Online] Available at: http://www.wareable.com/fitness-trackers/heart-rate-monitor-accurate-comparison-wrist (2015).

[11] “It’s easier to live healthier and achieve more.” [Online] Available at: https://www.microsoft.com/microsoft-band/en-gb/features (2015).

[12] D. Rubino “This is how often the Microsoft Band checks your heart rate” [Online] Available at: http://www.windowscentral.com/how-often-microsoft-band-checks-your-heart-rate (2015).

[13] V. Palladino “Who Has the Most Accurate Heart Rate Monitor?” [Online] Available at: http://www.tomsguide.com/us/heart-rate-monitor,review-2885.html (2015).

[14] The Healthline Editorial Team, “Hypothalamus” [Online] Available at: http://www.healthline.com/human-body-maps/hypothalamus (2015).

[15] T.Mojidra “Arduino Temperature Sensor LM35” [Online] Available at: http://www.instructables.com/id/ARDUINO-TEMPERATURE-SENSOR-LM35/ (2014).

[16] J. Pugh, “Ultra-Thin Sensor Bonds Directly To Skin To Continuously Monitor Temperature” University of Illinois, [Online] Available at: http://www.psfk.com/2013/09/ultrathin-wearable-thermometer.html (2013).

[17] “First Style in The World Fashion Test Body Temperature Stainless Steel Temperature Ring” [Online] Available at: http://www.miniinthebox.com/first-style-in-the-world-fashion-test-body-temperature-stainless-steel-temperature-ring_p1769792.html (2014).

[18] S.M “Smoothing” [Online] Available at: https://www.arduino.cc/en/Tutorial/Smoothing (2015).

[19] A. Gawande, *Being Mortal* ISBN: 978-1-84668-582-8 (Metropolitan Books), 6 (2014).

[20] M. Mosely, “Are Health Tests Really A Good Idea?” *(BBC Horizon, August 2015).*

[21] Shigehito Iguchia, Kohji Mitsubayashib, Takayuki Ueharac, Mitsuhiro Ogawa, “A wearable oxygen sensor for transcutaneous blood gas monitoring at the conjunctiva”, Sensors and Actuators B **108** , 733–737 (2005).

[22] B. Schyrr, S. Paschec, E. Scolana, R. Ischer, D. Ferrarioa, J. A. P, G. Voirina, “Development of a polymer optical fiber pH sensor for on-body monitoring application”, Sensors and Actuators B **194**, 238–248 (2014).

[23] L. Atallah, B. Lo, R. King, and GZ. Yang, “Sensor Positioning for Activity Recognition Using Wearable Accelerometers.” IEEE Transaction on Biomedical Circuits and systems, **5**, 320-329 (2011).

[24] PB. Adamson, WT. Abraham, M. Aaron, J. M Jr Aranda, R. C. Bourge, A. Smith, L. W. Stevenson, J. G. Bauman and J. S. Yadav. “Champion trial rationale and design: the long-term safety and clinical efficacy of a wireless pulmonary artery pressure monitoring system.” US National Livrary of Medicine, **17**, 3-10 (2011).

[25] J. E. Pandolfino, JE. Richter, T. Ours, J. M. Guardino, J Chapman, and PJ. Kahrilas, “Ambulatory Esophageal pH Monitoring Using a Wireless System.” The American Journal of Gastroenterology, **98**, 740-749 (2003).

[26] Withings, “What does SpO2 mean? What is the normal blood oxygen level?” [Online] Available at: https://withings.zendesk.com/hc/en-us/articles/201494667-Whatdoes-SpO2-mean-What-is-the-normal-blood-oxygen-level- (2015).

[27] R. Ortega, C. Hansen, K. Elterman and A. Woo, “Pulse Oximetry” The New England Journal of Medicine. [Online] Available at: https://www.youtube.com/watch?v=2v3rae-73jc. (2014).

[28] G. Sagar, “Introduction to Pulse Oximetry” [Online] Available at: http://chips.ece.iisc.ernet.in/images/a/a1/Pulse_oximetry.pdf. 1 (2012).

[29] AnaesthesiaUUK, “Principles of pulse oximetry” [Online] Available at: http://www.frca.co.uk/article.aspx?articleid=332

[29] A. Nobuyuki, N. Yasuhiro, T. Taiki, Y. Miyae, M. Kiyoko and H. Terumasa, “Trial of Measurement of Sleep Apnoea Syndrome with Sound Monitoring and SpO2 at home.” 66-69 (2012).

[30] A. Kishimoto, O. Tochikubo, K. Ohshige, A. Yanaga, “Ring-shaped pulse oximeter and its application: measurement of SpO2 and blood pressure during sleep and during flight.” Clin Exp Hypertens **27**, 279-88 (2005).

[31] Y.L.Zheng, X. R. Ding, Poon, C.C.Y, B.P.L. Lo, H. Zhang, X.L.Zhou, G.Z.Yang, N. Zhao and Y.T. Zhang, “Unobtrusive Sensing and Wearable Devices for Health Informatics.” Biomedical Engineering, IEEE **61**, 538-1554 (2014).

[32] J. Solà, S. Castoldi, O. Chételat, M. Correvon, S. Dasen, S. Droz, N. Jacob, R. Kormann, V. Neumann, A. Perrenoud, P. Pilloud, C. Verjus and G. Viardot, “SpO2 Sensor Embedded in a Finger Ring: design and implementation.” Conf Proc IEEE Eng Med Biol Soc. **1**, 4295 – 4298 (2006).

[33] F. Adochiei, C. Rotariu, R. Ciobotariu and H. Costin, “A Wireless Low-Power Pulse Oximetry System for Patient Telemonitoring.” Sensors and Actuators B **7** 1-4 (2011).

[34] M. Rothmaier, B. Selm, S. Spichtig, D. Haensse and M. Wolf, “Photonic textiles for pulse oximetry.” Optics Express, **16**, 12973-12986 (2008).

[35] S. M. Park, JY. Kim, KE. Ko, IH. Jang and Kwee-Bo Sim, “Real-Time Heart Rate Monitoring System based on Ring-Type Pulse Oximeter Sensor.” J Electr Eng Technol **8** 376-384 (2013).

[36] Y. Wu, C.S Chang, Y Sawaguchi, WC. Yu, MJ. Chen, JY. Lin, SM. Liu, CC. Han, WL Huang and CY Su, “A Mobile-Phone-Based Health Management System. Computers in Industry”, **69**, 3-11 (2015).

[37] UCSB ScienceLine, “Why is blood red?”, Availiable from: http://scienceline.ucsb.edu/getkey.php?key=2419. (2015).

[38] W. Nahm and H. Gehring, “Non-invasive in vivo measurement of blood spectrum by time-resolved near-infrared spectroscopy.” Sensors and Actuators B **29** 174-179 (1995).

[39] Public Lab “Foldable Mini-Spectrometer”, [Online] Available at: https://publiclab.org (2015).

[40] Texas Advanced Optoelectronic Solutions, “TCS3200, TCS3210 Programmable Color Light-To-Frequency Converter” 4 (2009).

[41] M. J. Campbell, editor. Swinscow TDV. In: Statistics at square one. Ninth Edition. Copyright BMJ Publishing Group (1997).

[42] “Connected Wrist Blood Pressure Monitor” [Online] Available at: http://www.ihealthlabs.eu/en/wireless-blood-pressure-monitors/8-wireless-blood-pressure-wrist-monitor.html (2015).

[43] A. Trafton, “Wearable blood pressure sensor offers 24/7 continuous monitoring” [Online] Available at: http://news.mit.edu/2009/blood-pressure-tt0408 (2009).

[44] M. Islam, F. Hasan, A. Mitul and M. Ahmad, “Development of a Noninvasive Continuous Blood Pressure Measurement and Monitoring System” International Conference on Informatics, Electronics & Vision, 1085 – 1090 (2012).

[45] S.T, “Math – mapping numbers” [Online] Available at: http://stackoverflow.com/questions/345187/math-mapping-numbers (2008).

[46] L. Bonsall, “Calculating the MAP” [Online] Available at: https://www.nursingcenter.com/NCBlog/December-2011/Calculating-the-MAP (2011).

[47] R. Pai “Heart Disease Health Center” [Online] Available at: http://www.webmd.com/heart-disease/electrocardiogram (2014).

[48] “An ECG Primer” Nursecom Educational Technologies 64-74 (2003).

[49] “The PQRST Heart Trace” [Online] Available at: http://www.cyberphysics.co.uk/topics/medical/heart/PQRST.html (2015).

[50] R. Klabunde, “Sequence of Cardiac Electrical Activation” [Online] Available at: http://www.cvphysiology.com/Arrhythmias/A003.htm (2008).

[51] D. Albert, “AliveCor Mobile ECG” [Online] Available at: http://www.alivecor.com/home (2015).

[52] S. Setayeshgar “Electrocadiogram (ECG) circuit for use with oscilloscopes” [Online] Available at: https://www.picotech.com/library/application-note/electrocardiogram-ecg-circuit-for-use-with-oscilloscopes (2014).